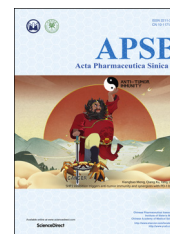




Chinese Pharmaceutical Association
Institute of Materia Medica, Chinese Academy of Medical Sciences

Acta Pharmaceutica Sinica B

www.elsevier.com/locate/apsb
www.sciencedirect.com



ORIGINAL ARTICLE

Design, synthesis and biological evaluation of chalcone analogues with novel dual antioxidant mechanisms as potential anti-ischemic stroke agents



Jiabin Wang^{a,b,†}, Lili Huang^{a,c,†}, Chanchan Cheng^{a,†}, Ge Li^{a,†},
Jingwen Xie^a, Mengya Shen^a, Qian Chen^a, Wulan Li^{a,d}, Wenfei He^a,
Peihong Qiu^{a,*}, Jianzhang Wu^{a,*}

^aChemical Biology Research Center, School of Pharmaceutical Sciences, Wenzhou Medical University, Wenzhou 325035, China

^bMunicipal Hospital Affiliated to Medical School of Taizhou University, Taizhou 318000, China

^cNingbo Medical Centre Li Huli Hospital, Ningbo 315041, China

^dCollege of Information Science and Computer Engineering, Wenzhou Medical University, Wenzhou 325035, China

Received 29 October 2018; received in revised form 3 December 2018; accepted 17 December 2018

KEY WORDS

Reactive oxygen species;
Cerebral ischemia-reperfusion injury;
Stroke;
Dual-antioxidant mechanism;
Chalcones;
Antioxidants;
Oxidative stress;
NRF2/ARE

Abstract Scavenging reactive oxygen species (ROS) by antioxidants is the important therapy to cerebral ischemia-reperfusion injury (CIRI) in stroke. The antioxidant with novel dual-antioxidant mechanism of directly scavenging ROS and indirectly through antioxidant pathway activation may be a promising CIRI therapeutic strategy. In our study, a series of chalcone analogues were designed and synthesized, and multiple potential chalcone analogues with dual antioxidant mechanisms were screened. Among these compounds, the most active **33** not only conferred cytoprotection of H₂O₂-induced oxidative damage in PC12 cells through scavenging free radicals directly and activating NRF2/ARE antioxidant pathway at the same time, but also played an important role against ischemia/reperfusion-related brain injury in animals. More importantly, in comparison with mono-antioxidant mechanism compounds, **33** exhibited higher cytoprotective and neuroprotective potential *in vitro* and *in vivo*. Overall, our findings showed compound **33** could

*Corresponding authors.

E-mail addresses: wjzwmc@126.com (Peihong Qiu), wjzwmu@163.com (Jianzhang Wu).

[†]These authors made equal contributions to this work.

Peer review under responsibility of Institute of Materia Medica, Chinese Academy of Medical Sciences and Chinese Pharmaceutical Association.

<https://doi.org/10.1016/j.apsb.2019.01.003>

2211-3835 © 2019 Chinese Pharmaceutical Association and Institute of Materia Medica, Chinese Academy of Medical Sciences. Production and hosting by Elsevier B.V. This is an open access article under the CC BY-NC-ND license (<http://creativecommons.org/licenses/by-nc-nd/4.0/>).

emerge as a promising anti-ischemic stroke drug candidate and provided novel dual-antioxidant mechanism strategies and concepts for oxidative stress-related diseases treatment.

© 2019 Chinese Pharmaceutical Association and Institute of Materia Medica, Chinese Academy of Medical Sciences. Production and hosting by Elsevier B.V. This is an open access article under the CC BY-NC-ND license (<http://creativecommons.org/licenses/by-nc-nd/4.0/>).

1. Introduction

Stroke, becoming one of the leading causes of morbidity and mortality across the world, brings increasingly great pressure to human lives. The large majority (85%) of strokes are ischemic stroke, that is, a stroke resulting from an occlusion of a major cerebral artery, and commonly it occurs in the middle cerebral artery^{1,2}. Although remarkable advances have been made in understanding the pathophysiology of cerebral ischemia, effective therapies are still a troubling aspect of human. To date, intravenous thrombolysis has been regarded as an effective strategy for the treatment of acute ischemic stroke³. However, rapid reperfusion accompanied by a large number of reactive oxygen species (ROS) by thrombolytic therapies, could exacerbate brain injury, namely cerebral ischemia-reperfusion injury (CIRI). Among a series of mechanisms related to the pathogenesis of CIRI, oxidative stress has been considered as the main reason^{4,5}. Oxidative stress, arising from the uncontrolled production of ROS beyond the neutralizing capacity of the various endogenous defense systems, including enzymatic and non-enzymatic matters, leads to cerebral cell apoptosis and neuronal damage^{6–8}. Therefore, exogenous supplementation of antioxidants with ROS scavenging activity would be a potential therapy to cerebral ischemia-reperfusion injury prevention.

Currently, there are two main classes of antioxidants based on the mechanism of inhibiting ROS: (1) compounds that can directly react with ROS are the so-called direct antioxidants, which have the ability to break down the procession of radical chain reactions, like edaravone, resveratrol, quercetin and so on^{9–11}. (2) Indirect antioxidants are compounds that do not directly react with ROS but are involved in activating cellular endogenous antioxidant signaling pathways and promoting the transcription of a broad range of cytoprotective genes to remove ROS, where KEAP1/NRF2/ARE is one of the important antioxidative signaling pathways. Many indirect antioxidants, such as TBHQ, curcumin and sulforaphane, that modify cysteine residues in the protein KEAP1, cause the dissociation of NRF2 from the inhibitory partner KEAP1 and facilitate NRF2 to translocate into the nucleus, where NRF2 binds to the antioxidant-responsive element (ARE) consensus sequence to activate the transcription of a panel of cytoprotective genes (phase II genes)^{9,11–13}. Despite extensive research on these two types of antioxidants, most antioxidants have been unsuccessful for clinically treating stroke except edaravone and other very few antioxidants. Moreover, direct and indirect antioxidants are not particularly effective in treating cerebral ischemia-reperfusion injury, which may be related to its own "birth defects". Direct antioxidants are short-lived, which may need to be continually provided to halt the process of cerebral ischemia-reperfusion injury¹¹. While stimulation of cellular endogenous antioxidant defense pathways by indirect antioxidants require a certain time, and during the period of time before activating the pathway, there is a risk that the brain would be irreversibly damaged by ROS

insult, since indirect antioxidants itself could not remove ROS immediately. Besides, up till now, there have been no reports about "dual-antioxidant mechanism action" for antioxidant therapy *via* both directly and indirectly scavenging ROS. Moreover, it is not clear whether antioxidants with dual-antioxidant mechanism may have a better prospect than the ones with mono-antioxidant mechanism for cerebral ischemia-reperfusion injury therapy. Herein, we hypothesized that antioxidant agents with ROS scavenging activity directly and indirectly may be more effective therapeutic strategies for stroke treatment.

Natural products and their synthetic analogues have been shown to be invaluable resources in drug discovery^{14–16}. Chalcones or (*E*)-1,2-diphenyl-2-propene-1-ones, make up a group of natural products that attach to the flavonoid family¹⁷. They consist in various of flowers, fruits, vegetables, and have been reported to possess many biological properties including antioxidant^{18–20}, antibacterial²¹, anticancer^{22,23}, antiangiogenic²⁴, and anti-inflammatory activities^{25,26}. Among all the biological activities, the antioxidant activity has been extensively studied. Given that a number of small molecules bearing polyhydroxyl groups exhibit a great efficacy in antioxidant activity due to their potent abilities to scavenge ROS directly^{27–30}, and it is well-known that the electrophilic α,β -unsaturated ketone moiety (Michael acceptor) on a chalcone can result in activation of the NRF2 pathway³¹, polyhydroxychalcones thus may be considered as monomers to study the potential of double antioxidative properties. In the study, we reported a number of novel (*E*)-3,4-dihydroxychalcone analogues as anti-ischemic stroke agents that attenuate oxidative stress by directly scavenging ROS and indirectly through KEAP1/NRF2/ARE pathway activation, leading to massive ROS elimination and subsequent inhibition of the ischemia-reperfusion-related brain injury in animals.

2. Results

2.1. Design and synthesis of chalcone analogues

Previous studies have demonstrated that chalcone-based compounds are involved in the indirect antioxidant effect *via* activation of the NRF2/ARE pathway³¹. Polyphenols are considered as an appropriate structural element for designing direct antioxidant compounds, especially compounds bearing 3,4-dihydroxyl substituents on benzene ring showed potent free radical scavenging effects³². Besides, the presence of the α,β -double bond on chalcone could increase the stabilization of the phenolic radical³². Therefore, chalcone analogues containing 3,4-dihydroxyl substituents may show effective direct and indirect antioxidant activities. In present study, a series of (*E*)-3,4-dihydroxychalcones and corresponding dimethoxychalcones derivatives as control compounds were synthesized. Furthermore, in order to explore whether 3,4-dihydroxyl substituents in the "A" or "B" ring of chalcones have different effects on antioxidant activity, different moieties

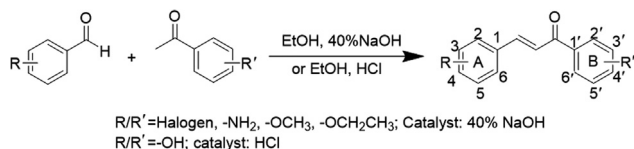
were introduced on one benzene ring, while another benzene ring retained the 3,4-dihydroxyl substituents.

The synthetic profiles of the compounds and their chemical structures are listed in Scheme 1 and Table 1. The target chalcone-based compounds were synthesized by the Claisen–Schmidt condensation with NaOH or HCl as catalyst in good yield by a known literature method^{33–35}. In summary, substituents such as halogen, amidogen, methoxyl and ethoxyl were catalyzed by NaOH, and others such as hydroxyl were catalyzed by HCl. The purity was determined by TLC, and the products were characterized by analysis and comparison of their spectral and physical data including HR-MS, ¹H NMR and ¹³C NMR. The color, melting point, HR-MS, ¹H NMR and ¹³C NMR spectrum of novel and unpublished compounds were presented in the chemical section.

2.2. Protection of chalcone derivatives from H₂O₂-induced damage in PC12 cells

Hydrogen peroxide (H₂O₂) as an endogenous cellular signaling molecule could generate exogenous free radicals immediately, which are able to induce lipid peroxidation, and proteins and nucleic acid oxidation, and ultimately lead to cell death^{36,37}. Therefore, we evaluated chalcone analogues as potential cytoprotective agents against H₂O₂-mediated cell damage in a neuron-like cell line, PC12 cells.

Pre-incubation with antioxidants for a long time (more than 6 h), the antioxidants could stimulate endogenous antioxidant defense systems against ROS^{38,39}. The cells were pretreated by the tested



Scheme 1 Synthesis of chalcone derivatives 1–41. Reagents and conditions: EtOH, 40% NaOH or HCl, room temperature, 12–24 h.

compounds for 24 h, and then treated with H₂O₂ insult could be accepted as an experimental method for studying antioxidant activity^{39–43}. Therefore, to study cytoprotection activity of compounds, the screening model of pre-incubation for 24 h was used in this test first. Quercetin, edaravone (ED) and TBHQ are well-known antioxidants, which are used as the positive controls. As shown in Fig. 1A, some (*E*)-3,4-dihydroxychalcones exhibited good protective efficacy, while only a few (*E*)-3,4-dimethoxychalcones displayed weak cytoprotection. Surprisingly, among these (*E*)-3,4-dihydroxychalcones, chalcones with 3,4-dihydroxyl groups on ring “A”, electron donating groups or electron withdrawing groups on ring “B”, all displayed potent cytoprotection. Moreover, compared with quercetin, ED and TBHQ, compounds **23**, **25**, **29**, **31**, **33**, **37**, **39** and **41** exerted greater cytoprotection effects. However, only compounds **7**, **13** and **19** bearing 3,4-dihydroxyl substituents on ring “B” had cytoprotection activity.

In general, due to the pretreatment with antioxidants for a short time (within 2 h) followed by H₂O₂ insult, there is not enough time to induce the expression of cytoprotective protein, and antioxidants may play cytoprotective effect by directly neutralizing ROS⁴⁴. Thus, we chose the screening model of compounds pre-incubation for 1 h to further study the free radical scavenging activity. Notably, all (*E*)-3,4-dihydroxychalcones were capable of relieving the cell injury induced by H₂O₂ insult, whereas the (*E*)-3,4-dimethoxychalcones exhibited no cytoprotection (Fig. 1B).

To further validate their direct free radical scavenging activity, 2,2-diphenyl-1-picrylhydrazyl (DPPH) assay was further applied in the test⁴⁵. As shown in Fig. 1C, as expected, chalcone analogues bearing 3,4-dihydroxyl substituents on ring “A” or “B” all exhibit significant ability to scavenge free radicals directly. In contrast, (*E*)-3,4-dimethoxychalcones were found to be inactive. The result was in line with the damage model with compounds pre-incubation for 1 h, which showed compounds might execute their cytoprotection through scavenging free radicals directly.

More interestingly, compound **21** showed cytoprotection activity only in the model of pre-incubation for 1 h, which suggested

Table 1 The structures of chalcone derivatives 1–41.

Compd.	R in A-ring	R' in B-ring	Compd.	R in A-ring	R' in B-ring
1	3,4-OH	3-OH	22	3,4-OCH ₃	3,5-F
2	3,4-OCH ₃	3-OH	23	4-OCH ₃	3,4-OH
3	3,4-OH	4-NH ₂	24	4-OCH ₃	3,4-OCH ₃
4	3,4-OCH ₃	4-NH ₂	25	3-OH, 4-OCH ₃	3,4-OH
5	3,4-OH	4-OCH ₃	26	3-OH, 4-OCH ₃	3,4-OCH ₃
6	3,4-OCH ₃	4-OCH ₃	27	2,4-OCH ₃	3,4-OH
7	3,4-OH	4-OCH ₂ CH ₃	28	2,4-OCH ₃	3,4-OCH ₃
8	3,4-OCH ₃	4-OCH ₂ CH ₃	29	2-OCH ₃	3,4-OH
9	3,4-OH	4-Cl	30	2-OCH ₃	3,4-OCH ₃
10	3,4-OCH ₃	4-Cl	31	2,3-OCH ₃	3,4-OH
11	3,4-OH	2-F	32	2,3-OCH ₃	3,4-OCH ₃
12	3,4-OCH ₃	2-F	33	2,5-OCH ₃	3,4-OH
13	3,4-OH	2-Cl	34	2,5-OCH ₃	3,4-OCH ₃
14	3,4-OCH ₃	2-Cl	35	4-Cl	3,4-OH
15	3,4-OH	4-F	36	4-Cl	3,4-OCH ₃
16	3,4-OCH ₃	4-F	37	3,4-Cl	3,4-OH
17	3,4-OH	3,4-F	38	3,4-Cl	3,4-OCH ₃
18	3,4-OCH ₃	3,4-F	39	3,4,5-OCH ₃	3,4-OH
19	3,4-OH	3,4-OCH ₃	40	3,4,5-OCH ₃	3,4-OCH ₃
20	3,4-OCH ₃	3,4-OCH ₃	41	3,4-OCH ₃	3,4-OH
21	3,4-OH	3,5-F			

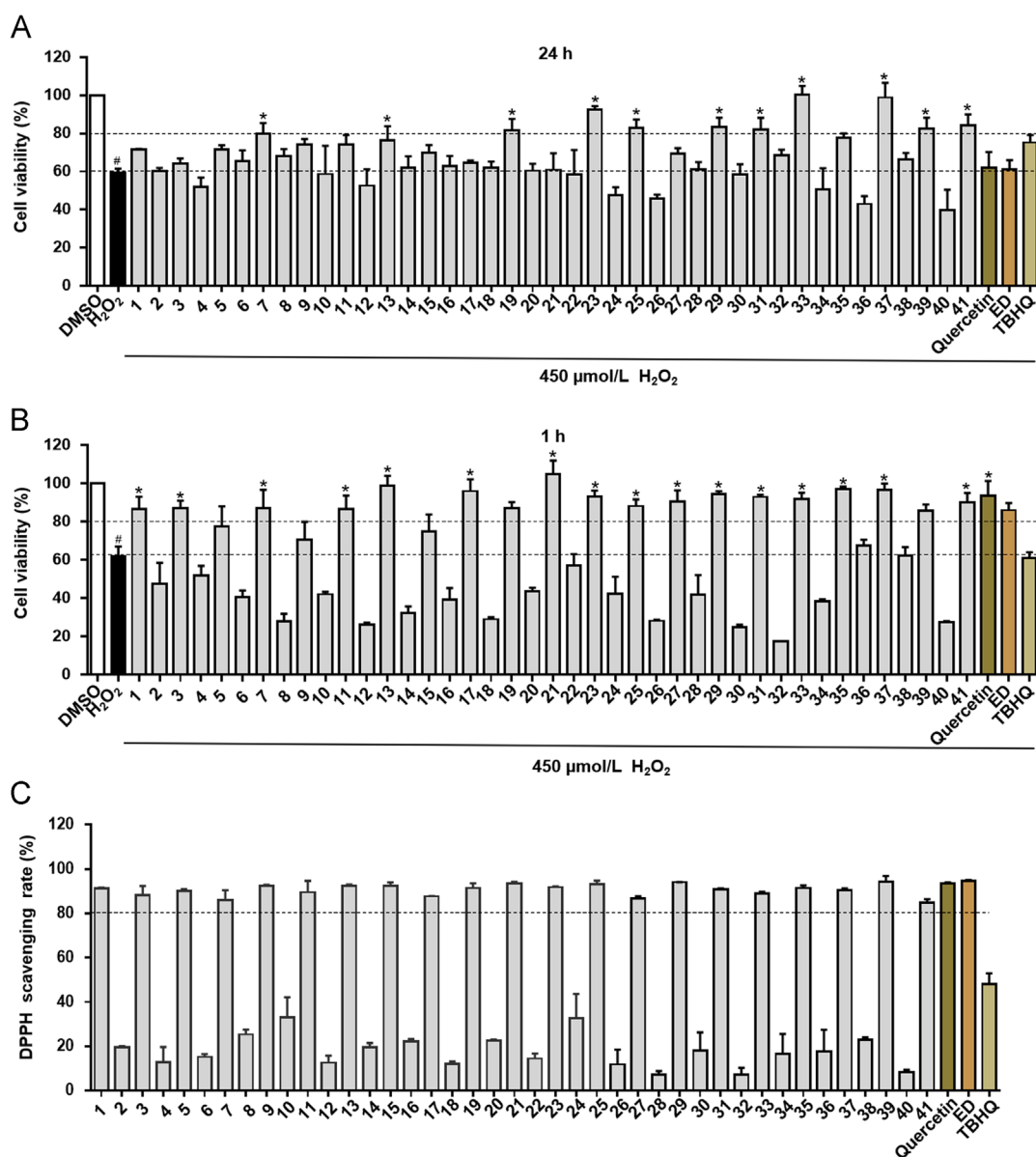


Figure 1 Compounds' cytoprotection on PC12 cells in H₂O₂ damage model and DPPH radical scavenging activities of chalcone analogues. PC12 cells were pretreated for 24 h (A) or 1 h (B) with chalcone analogues (10 μmol/L), then another 24 h exposure in H₂O₂ (450 μmol/L), finally determined by the MTT assay. The viability of untreated cells is defined as 100%. (C) DPPH radical scavenging rate of chalcone derivatives (20 mg/L). Data are expressed as the mean ± SD (*n* = 3). #*P* < 0.05 significantly different from control group, **P* < 0.05 significantly different from H₂O₂ group.

that its antioxidant mechanism may *via* directly removing free radicals. Compounds **7**, **13**, **19**, **23**, **25**, **27**, **29**, **31**, **33**, **35**, **39** and **41** were found to have good advantages for cytoprotection at both time points, and thus these compounds may act as both “direct” and “indirect” antioxidants.

2.3. Compound **33** with dual-antioxidant mechanism showed better antioxidant activity than compounds with mono-antioxidant mechanism *in vitro*

So far, compared with antioxidants with mono-antioxidant mechanism, there are no reports about whether those with dual-antioxidant mechanism may have better drug prospects. Based on the promising cytoprotection activity, compound **33** could be

considered as a direct and indirect antioxidant. Thus, **33** was selected as the candidate compound with dual-antioxidant mechanism for further investigation. In addition, the molecules that have similar structure to **33** are chosen as control compounds with mono-antioxidant mechanism. Compound **21** mentioned above may be a free radical scavenger. Furthermore, (*E*)-3,4-dimethoxy-chalcones without phenolic hydroxy showed no effective cytoprotection activity in the study, which suggested that there may be no indirect antioxidants. In our previous study, chalcone derivatives were found to act as antioxidants by activating the antioxidant NRF2 signaling pathway, and compound **1b** without phenolic hydroxy pretreatment for 24 h had an ability to protect against H₂O₂-triggered cell apoptosis⁴³ (Supporting Information Fig. S1). After pre-incubation with **1b** for 1 h followed by H₂O₂ insult, the population of viable cells did not

increase (Supporting Information Fig. S1), which means **1b** may execute the antioxidant activities mainly through activating antioxidant signaling pathway. Immunofluorescence experiments also revealed that NRF2 nuclear translocation was activated by compounds **33** and **1b**, rather than by compound **21** (Fig. 3A and Supporting Information Fig. S2). In order to confirm whether compounds **33**, **1b** and **21** could stimulate the related protein coding genes expression in the NRF2-ARE signaling pathway, Western blot experiments were further determined. As showed in Fig. 2C, compound **21** could not upregulate HO-1 protein expression in PC12 cells, while both compounds **33** and **1b** could elevate HO-1 level. Therefore, according to the above results, compound **33** was proven as a both “direct” and “indirect” antioxidant, while compounds **21** and **1b** were deemed as a free radical scavenger and an activator of cellular antioxidant pathway, respectively, and were used as the control compounds with mono-antioxidant mechanism.

Generally speaking, ideal antioxidant agents have lower toxicity, so the cytotoxicity of compounds (**1b**, **21** and **33**) toward the PC12 cells were assessed. As shown in Fig. 2A, there is no apparent cytotoxicity of the tested compounds at 10 $\mu\text{mol/L}$. To compare the antioxidant activity of these compounds, PC12 cells were pretreated with compounds **1b**, **21** and **33** for 10 time points from 1 to 24 h followed by H_2O_2 challenge. The results showed that compound **33** exhibited potent cytoprotection throughout the incubation time, while compounds **21** and **1b** were active only when pretreated for 1–10 h and 9–18 h, respectively, which indicated that compound **33** has better antioxidant activity (Fig. 2B). To explore the different mechanisms of antioxidant activity among compounds **1b**, **21** and **33**, the expression of HO-1 protein at 0, 2, 6, 12, 18 and 24 h after treatment with compounds in PC12 cells was further determined. As shown in Fig. 2C, **33** and **1b** both started to activate the expression of HO-1 at 12 h and could last continuously to 24 and 18 h, respectively, whereas **21** could not induce HO-1 expression. Therefore, these data collectively demonstrated that **21** generally relies on the facile ability of phenols to be oxidized to wield its primary cytoprotection effect, while **1b** was involved in endogenous cellular NRF2 signaling pathway to diminish oxidative damage. Taken together, compared with mono-antioxidant mechanism compound, **33** displayed better protection *in vitro*.

In order to further determine the potential interest of **33** as a cytoprotective agent, PC12 cells were pretreated with **33** for 1 or 24 h, and incubated with H_2O_2 for another 24 h. As shown in Fig. 2D, the population of viable cells increased in a dose-dependent manner. The burst of ROS is unavoidable when cells are stimulated with H_2O_2 . To confirm the ROS scavenging activity of **33**, we further determined the content of ROS after H_2O_2 insult. As shown in Fig. 2E, pretreatment of the cells with **33** for 1 or 24 h remarkably reduced the ROS accumulation. Malondialdehyde (MDA), a byproduct of polyunsaturated fatty acid peroxidation caused by ROS, is regarded as a significant biomarker of oxidative stress⁴⁶. It is found that addition of **33** for 1 or 24 h significantly reduced the MDA in a dose-dependent manner (Fig. 2F). Consequently, compound **33** significantly protected PC12 cells from H_2O_2 -induced cell injury.

2.4. Activation of NRF2-ARE pathway is responsible for the antioxidant activities of compound **33**

When NRF2 is activated, it translocates into the nucleus and thus further exerts its transcriptional function. Hence, we examined

whether compound **33** can induce the nucleus translocation of NRF2 in PC12 cells by immunofluorescence. ED and TBHQ were used as positive controls. The blue and red staining represent nuclei and NRF2, respectively, and merge represents both. As shown in Fig. 3A, compared to the blank control group, there was strong fluorescent light in the nucleus, clearly showing that **33** could induce NRF2 translocation and concentration in the nucleus. Authentically, the similar phenomenon occurred when treated with TBHQ and ED. The results supported that **33** was able to promote NRF2 to accumulate in the nuclei.

NRF2 can initiate the transcription of phase II genes, the expression of *GCLC* and *HO-1* were further determined. First of all, the *GCLC* and *HO-1* mRNA expression levels induced by **33** were investigated by RT-PCR. As shown in Fig. 3B–C, **33** clearly increased the *GCLC* and *HO-1* mRNA levels in a dose-dependent manner. The data showed compound **33** treatment could effectively activate the transcription of NRF2-driven antioxidant genes. Furthermore, to elucidate the mechanism of **33**, Western blot assays were used to determine the expression levels of *GCLC* and HO-1. After PC12 cells were treated with **33** at 2.5, 5 and 10 $\mu\text{mol/L}$ levels for 24 h, the expression of *GCLC* and HO-1 protein enhanced in a concentration-dependent manner (Fig. 3D). Especially, **33** at 5 $\mu\text{mol/L}$ exhibited much stronger promoting effects than TBHQ at 10 $\mu\text{mol/L}$.

To make sure if the expression of *GCLC* and HO-1 caused by the **33** is responsible for the cytoprotective effects against H_2O_2 -derived oxidative cell death, BSO and ZnPP, which are specific inhibitors of *GCLC* and HO-1 respectively, were utilized in this study^{43,44,47}. As shown in Fig. 3E, after PC12 cells were pretreated with ZnPP (15 $\mu\text{mol/L}$) or BSO (10 $\mu\text{mol/L}$) for 1 h, there is no obvious adverse effects on the viability of PC12 cells. Applying **33** alone raised the cell viability, while BSO or ZnPP all can cause a dramatic decrease in cell viability induced by **33**. These results suggested that promotion NRF2 translocation into the nucleus and further induction of *GCLC* and HO-1 expression had a significant function in hindering oxidative stress, and at least partly, explaining the antioxidant activity of **33**. In all, according to the results *in vitro*, it seems that compound **33** is an ROS scavenger and an activator of cellular intrinsic KEAP1/NRF2/ARE antioxidant pathway at the same time.

2.5. Protective effect of compound **33** was more pronounced than that of mono-antioxidant mechanism compound on cerebral ischemia-reperfusion injury

Inspired by the results above, **33** showed significantly higher protection of PC12 cells against oxidative insults through dual antioxidant mechanisms *in vitro*. However, it is still not clear that whether **33** has a better protection than the mono-antioxidant mechanism compound for inhibiting cerebral ischemia-reperfusion injury. Hence, the neuroprotective activity of **33** *in vivo* was further investigated in a rat model of transient focal cerebral ischemia by intraluminal occlusion of the middle cerebral artery (MCAO), which was considered to be the most common reason for inducing I/R-related brain injury in the clinic⁴⁸. Considering that administration of various drugs by intraperitoneal or intravenous injection exists different absorption, distribution, metabolism and excretion (ADME), which could disturb their efficacy, the anti-ischemic stroke effects of **33**, **21** and **1b** were evaluated by pre-injection into lateral ventricles in order to exclude the effect of peripheral pharmacokinetics of drugs. The infarct size of individual rat was evaluated by the 2,3,

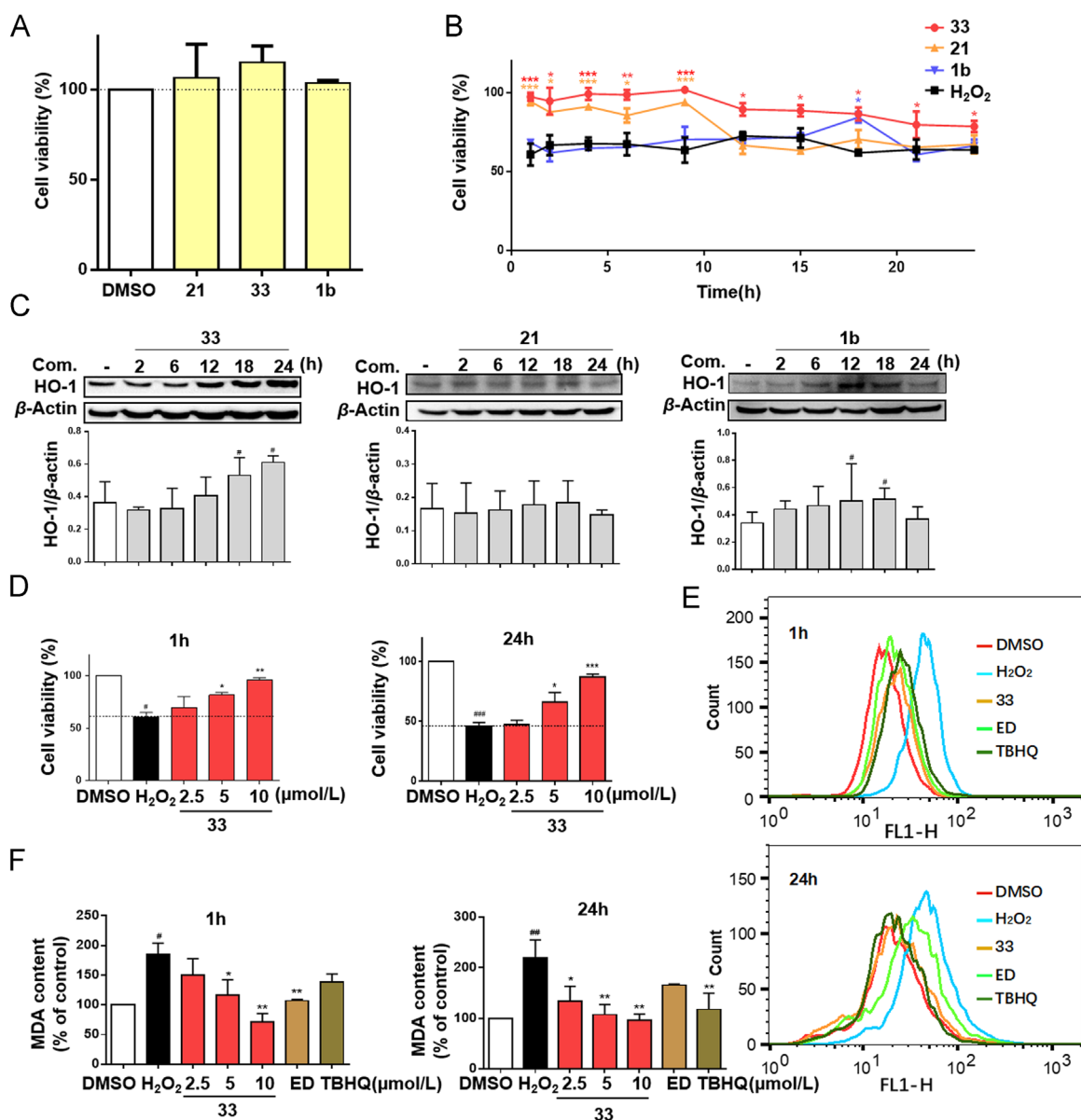


Figure 2 The cytoprotective effects of **33** on PC12 cells subjected to H_2O_2 . (A) Cytotoxicity screening of **33** in PC12 cells. The cells were treated with $10\ \mu\text{mol/L}$ of **21**, **33** and **1b** for 24 h, and the cytotoxicity of compounds were determined by the MTT assay. (B) Protection of compound **33** against H_2O_2 -induced PC12 cell damage. PC12 cells were incubated with $10\ \mu\text{mol/L}$ of **33**, **21**, **1b** for 1, 2, 4, 6, 9, 12, 15, 18, 21 and 24 h before exposed to H_2O_2 ($450\ \mu\text{mol/L}$) for additional 24 h. Then the cell viability was determined by MTT assay. (C) Elevating the expression level of protein HO-1 by **33**. PC12 cells were incubated with **33** ($10\ \mu\text{mol/L}$), **21** ($10\ \mu\text{mol/L}$), **1b** ($10\ \mu\text{mol/L}$) for 2, 6, 12, 18 and 24 h, and the HO-1 was determined by Western blot experiment. (D) **33** protected PC12 cells from H_2O_2 -induced cell injury. PC12 cells were pretreated with **33** in different doses (2.5 , 5 and $10\ \mu\text{mol/L}$) for 1 or 24 h, then treated with $450\ \mu\text{mol/L}$ H_2O_2 for 24 h, and determined by the MTT assay. (E) **33** decreased ROS level in H_2O_2 -treated PC12 cells. PC12 cells were pre-treated with $10\ \mu\text{mol/L}$ of **33**, ED or TBHQ, then treated with H_2O_2 for 4 h, and the ROS level was measured by flow cytometry. (F) Protection of compound **33** by reducing MDA. PC12 cells were pre-incubated with **33** at 2.5 , 5 and $10\ \mu\text{mol/L}$, ED ($10\ \mu\text{mol/L}$) or TBHQ ($10\ \mu\text{mol/L}$) for 1 or 24 h, then treated with $700\ \mu\text{mol/L}$ H_2O_2 for 16 h, finally determined by the manufacturer's instructions. Data are expressed as the mean \pm SD ($n=3$). $###P<0.001$, $##P<0.01$, $\#P<0.05$ significantly different from control group, $***P<0.001$, $**P<0.01$, $*P<0.05$ significantly different from H_2O_2 group.

5-triphenyltetrazolium chloride (TTC) staining⁴⁹. As illustrated in Fig. 4A–B, as expected, there were no obvious neuronal abnormality in the sham group, whereas the infarct area in the model group and vehicle group of rats significantly increased, as shown in the white region of rat brain sections. But, intracerebroventricular administration of **33** markedly reduced the infarct sizes of I/R rats. Additionally, treatment with **33** improved the neurologic scoring in the brains from

ischemic rats. The addition of **21** and **1b** were found to show weak protective effects on infarction damage, respectively (Fig. 4C). Therefore, the effect of **33** was more pronounced than that of **21** and **1b**, which was in accordance with the cell-based results. It suggested that the compound with dual antioxidant mechanism may have more potential for the treatment of ischemic brain damage compared with the compound with mono-antioxidant mechanism.

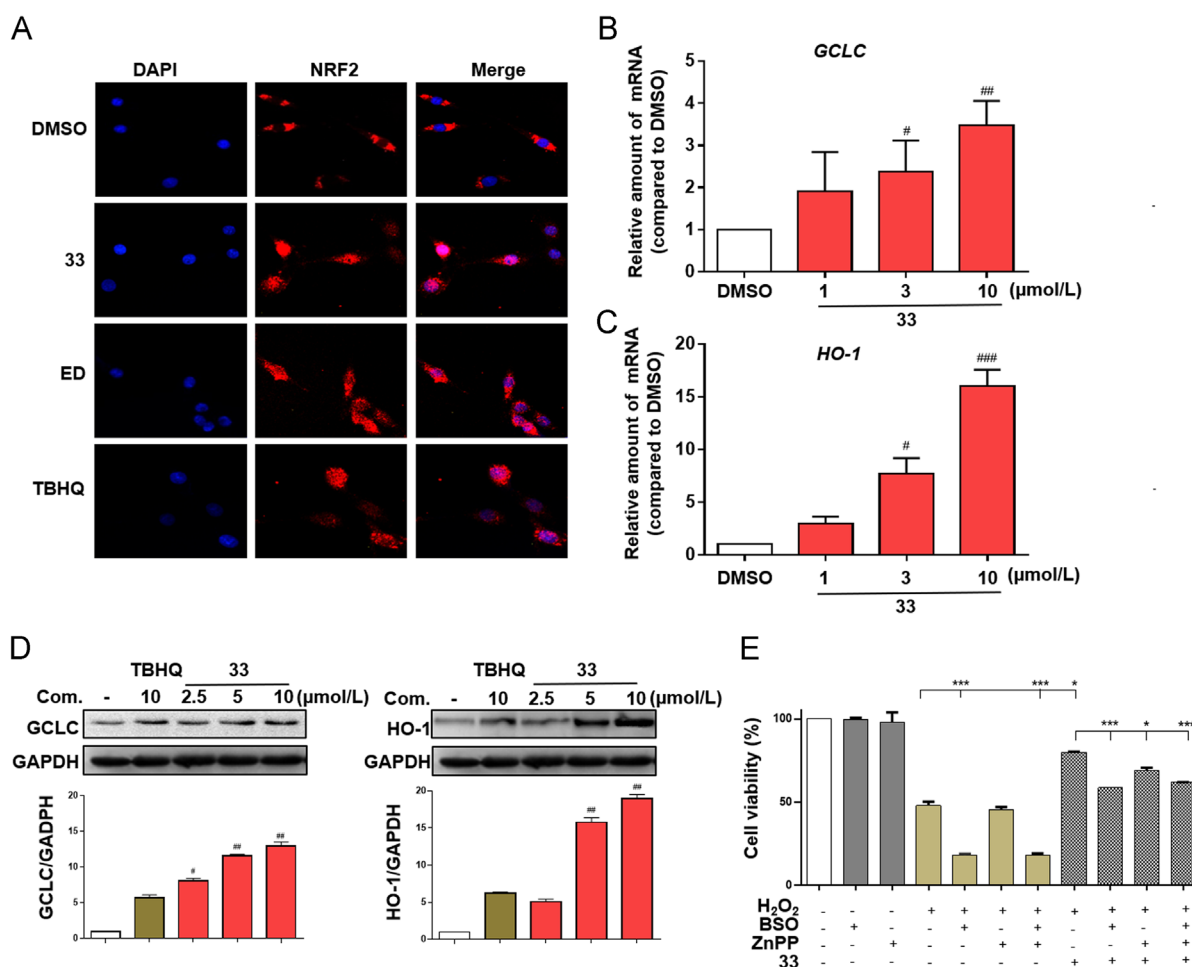


Figure 3 Compound **33** activated the antioxidant defense system in PC12 cells. (A) **33** promoted NRF2 translocation into the nucleus. PC12 cells were incubated with **33**, ED and TBHQ at 10 μmol/L for 6 h, and then stained with NRF2 antibody and DAPI. (B) and (C) **33** induced the mRNA expression of *GCLC* and *HO-1*. PC12 cells were incubated with **33** in different doses for 24 h and then evaluated the mRNA level of *GCLC* and *HO-1* by RT-PCR experiment. (D) **33** induced the protein expression of GCLC and HO-1. PC12 cells were incubated with **33** at 2.5, 5 and 10 μmol/L, TBHQ at 10 μmol/L for 24 h, and the GCLC and HO-1 were determined by Western blot experiment. (E) BSO or ZnPP diminished the protected effect of **33** on H₂O₂ induced cell damage. PC12 cells were incubated with GCLC inhibitor BSO or HO-1 inhibitor ZnPP for 1 h, then treated with **33** (10 μmol/L) for 24 h and exposed to H₂O₂ (450 μmol/L) for additional 24 h. Finally, MTT assay measured the OD values in 490 nm. Data are expressed as the mean ± SD (n=3). ###P<0.001, ##P<0.01, #P<0.05 significantly different from control group, ***P<0.001, **P<0.01, *P<0.05.

2.6. Therapeutic effects of compound **33** on cerebral ischemia-reperfusion injury

To date, in addition to preventative therapies for stroke, there has been a more important need to develop effective therapeutic therapies in clinic. Within 3–6 h after stroke onset has been considered as prime time against brain ischemia^{50,51}. Therefore, we next evaluated the therapeutic characteristics of **33** in exerting its effectiveness 3 and 6 h following ischemia-reperfusion injury. To demonstrate the cerebral therapeutic effects of compound **33**, MCAO rat model was also used in this study. Edaravone as a direct antioxidant has been demonstrated to show therapeutic effects on ischemic stroke in the clinic and was used as positive control. Similarly, from the results of TCC staining and neurological scoring, **33** showed more significant therapeutic effect than edaravone when administration conducted 3 or even 6 h after I/R induction (Fig. 5A–C).

Cerebral ischemia is known to produce severe behavioral deficits, and bilateral cerebral artery occlusion (BCAO), as another model, was applied for evaluating its protection activity by open field test to estimate locomotor activity of the tested mice. Their total distance of the in-between 5 min traveled during the observation period was collected and analyzed. As shown in Fig. 5D–E, no obvious ischemia-induced barriers to behavior were observed in sham-operated group. However, the I/R model and vehicle-treated group of mice showed prominent behavioral deficits and the locomotor activity decreased markedly compared with the sham-operated group. In contrast, the neurobehavioral function of compound **33** or edaravone treated mice had obviously improved at 3 h after cerebral ischemia-reperfusion injury. Especially, when intraperitoneal injection of **33** even 6 h after I/R onset, it still had dramatic improvement in exercise behavior, which had even much stronger protective effect than edaravone. In all, these data showed that compound **33** could emerge as a promising anti-ischemic stroke drug candidate.

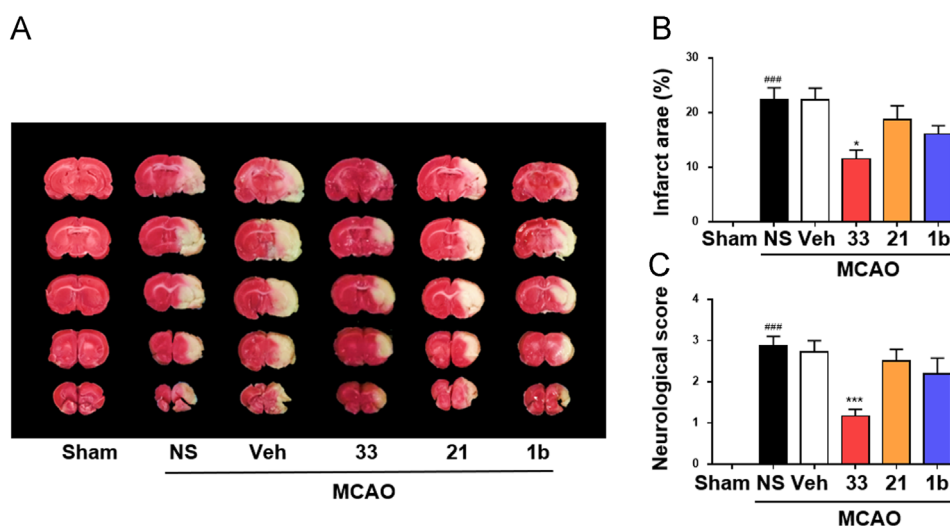


Figure 4 Protective effect of compounds **33**, **21** and **1b** on brain infarct after 72 h reperfusion. (A) TTC staining analysis of the infarcted brain regions. (B) Quantitative analysis of the infarcted brain regions. The ratios of infarct area to whole brain areas in individual rats were calculated. (C) Quantitative analysis of neurological score. Cerebral infarction in Sham-operated (Sham) or MCAO-reperfusion rats from a representative animal that received normal saline (NS), Veh (polymer:DMSO:distilled water at 50 mg:1 mL:3 mL), or **33**-nanoparticles (0.2 mg/kg), **21**-nanoparticle (0.2 mg/kg), and **1b**-nanoparticles (0.2 mg/kg) intracerebroventricularly 2 h before MCAO. Data are expressed as the mean \pm SD ($n=3$). $###P < 0.001$ significantly different from Sham group, $***P < 0.001$, $*P < 0.05$ significantly different from control group.

3. Discussion

Excessive production of ROS is known to lead to acute ischemic injury in various organs, and numerous studies have demonstrated antioxidant therapy is considered as an effective strategy in ischemic disorders^{52–56}. For the current status of antioxidants, this research not only offers novel dual-antioxidant mechanism strategies and concepts on oxidative stress-related diseases treatment, but also provides promising candidate antioxidant drugs with dual-antioxidant mechanism.

Attenuation acute ischemic injury can be mediated by direct and indirect antioxidants. Among them, *N*-acetylcysteine (NAC) has been extensively used as a powerful ROS scavenger and potent neuroprotective actions for the treatment of acute ischemic stroke and rhabdomyolysis-induced acute kidney injury in animal models, respectively^{57,58}. As for indirect antioxidants, such as tert-butylhydroquinone, which has been shown to enhance NRF2 signaling activity and protect against ROS in various brain cells *in vitro*^{59–61}. Comparing the direct and indirect antioxidants, the study of Jokod showed that indirect antioxidants were more beneficial for cytoprotection than direct antioxidants *in vitro*⁶². Moreover, some antioxidants, including melatonin and resveratrol, appear to play a dual-antioxidant protective role as direct and indirect antioxidants^{63–65}.

Up till now, there was no study about whether the compounds with dual-antioxidant mechanism may have a better prospect than the ones with single-antioxidant mechanism in acute ischemic stroke. In the present study, compound **33** not only scavenged ROS directly, but also activated NRF2 pathway, and thus it could be considered a both direct and indirect antioxidant. Notably, when PC12 cells were pretreated with **33** for 10 time points from 1 to 24 h followed by H₂O₂ insult, **33** exhibited excellent cytoprotection at all the incubation time. For mono-antioxidant compounds, when pretreated with compound **21** as direct antioxidant, the cytoprotection against H₂O₂ lasted 1–10 h, and when pretreatment with compound **1b** as indirect antioxidant showed

cytoprotection only for 9–18 h. Furthermore, interestingly, compound **33** showed a preferable role for neuroprotecting against cerebral ischemia-reperfusion injury in animal models compared with compounds **21** and **1b**. Taken together, all results suggested that drugs with dual-antioxidant mechanism might be more pronounced than that with single-antioxidant mechanism, which could provide novel and promising strategies and concepts for drug research on antioxidant and stroke treatment.

Natural or synthetic bioactive chalcones have attracted enormous attention in drug exploration due to their low toxicity and various biological activities, especially since they were found to prevent oxidative stress-induced neurodegenerative disorders. For instance, xanthohumol showed protection against oxidative damage in PC12 cells *via* activating NRF2 enzymes³⁸. The study of Jeon also demonstrated chalcone derivatives displayed neuroprotective effects against oxidative stress-induced apoptosis in SH-SY5Y cells⁶⁶. In our present study, after treatment with chalcone analogue **33** in both BCAA and MCAO models, all exhibited significant protective effects. Divertingly, compound **33** exerted higher central protection than edaravone at the same dose when administration conducted 3 or even 6 h after I/R induction. Therefore, **33** could serve as a potent candidate antioxidant drug for anti-ischemic stroke drug research and other ischemic disorders treatment.

Phenolic compounds possess high antioxidant activity and are potent regulators of cellular redox status, which have been frequently considered as potent antioxidants. Natural chalcones bearing 3,4-dihydroxyl groups, such as butein, sappanchalcone and okanin, are particularly effective antioxidants^{67–69}. Chiruta et al.⁷⁰ reported chalcone derivatives containing catechol group contributed to neuroprotective activity and maintenance of GSH. In addition, Dziedzic et al.⁷¹ revealed that molecules bearing ortho-dihydroxyl possess significantly higher antioxidant activity than those bearing no such functionalities, which may be due to the abstraction of the two hydrogen atoms of the ortho-position hydroxyls respectively, to form a quinone structure.

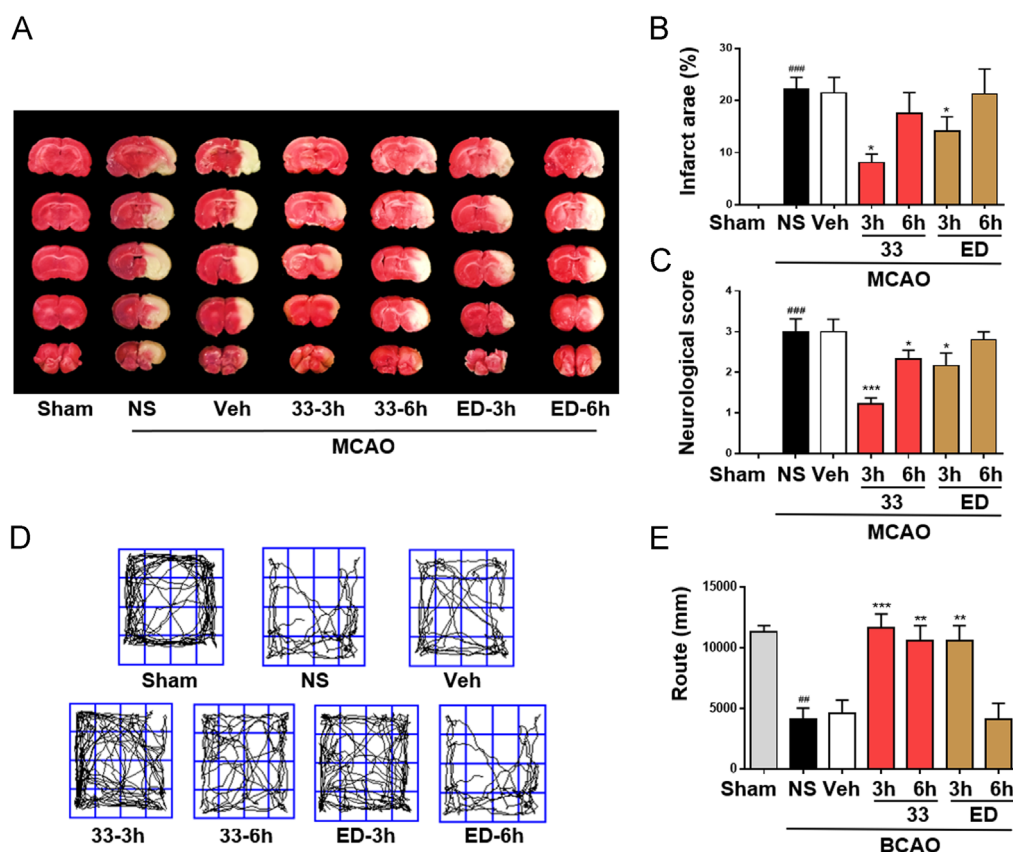


Figure 5 Therapeutic effect of compound **33** on cerebral ischemia-reperfusion injury. (A) TTC staining analysis of the infarcted brain regions. Quantitative analysis of the infarcted brain regions (B) and neurological score (C). (D) and (E) The locomotion trace of the mice in the chamber for a period of 5 min. All animals were divided into seven groups: sham-operated group, NS group, Veh (Cremophor:PBS at 3:97) group, **33** (15 mg/kg, 3 h) + MCAO group, **33** (15 mg/kg, 6 h) + MCAO group, ED (15 mg/kg, 3 h) + MCAO group and ED (15 mg/kg, 6 h) + MCAO group. All rats received drug intraperitoneally 3 or 6 h after MCAO. Data are expressed as the mean \pm SD ($n=3$). ### $P < 0.001$, ** $P < 0.01$, * $P < 0.05$ significantly different from Sham group, *** $P < 0.001$, ** $P < 0.01$, * $P < 0.05$ significantly different from control group.

Benayahoum et al.⁷² reported the great reactivity of the ortho-dihydroxyl system is possibly due to the smaller dissociation energy of the O-H bond. Moreover, compounds including 3,4-dihydroxyl groups on benzene ring were found to be more potent antioxidant than resveratrol⁷³. Hence, chalcone derivatives bearing 3,4-dihydroxyl are favorable for the development of effective antioxidants.

In our study, chalcone analogues bearing 3,4-dihydroxyl groups on ring "A" or ring "B" were designed and synthesized. After PC12 cells were pretreated with (*E*)-3,4-dihydroxychalcones for a short time (1 h) followed by H₂O₂ challenge, all compound markedly promoted cell viability, while chalcone derivatives bearing a hydroxyl group or no hydroxyl group remained inactive. Additionally, the results of DPPH assay confirmed the above results, which suggested the (*E*)-3,4-dihydroxychalcones could scavenge ROS directly. When pretreated for 24 h, there are many 3,4-dihydroxychalcone derivatives showing advantageous cytoprotection. Interestingly, compared with 3,4-dihydroxyl groups on ring "B", chalcone analogues with 3,4-dihydroxyl groups on ring "A" all showed significant cytoprotection and had a great improvement on antioxidant capacity, which suggested that the presence of 3,4-dihydroxyl groups on ring "A" may be good for antioxidant activity. Given that the number of (*E*)-3,4-dihydroxychalcones is limited, further research is needed to establish a clearer quantitative structure-activity relationship between

structure and cytoprotection with more compounds. Furthermore, compound **33** containing 3,4-dihydroxyl groups on ring "A" with the best antioxidant activity was screened out, and further study showed that **33** could activate NRF2 pathway. So hypothetically, stimulating NRF2 pathway may also occurred in other cytoprotective chalcone analogues containing 3,4-dihydroxy groups on "A" ring. Taken together, chalcone analogues with 3,4-dihydroxyl groups on ring "A" presented important neuroprotective activity via directly scavenging ROS and indirectly through NRF2 pathway activation. Therefore, (*E*)-3,4-dihydroxychalcone may be considered as a promising structural element for designing antioxidant compounds with dual-antioxidant mechanism.

4. Conclusions

In the research of antioxidant field, there are no researches on the antioxidant agents with novel dual-antioxidant mechanism of directly scavenging ROS and indirectly through activation of antioxidant pathway. It is also unclear whether antioxidants with dual antioxidant mechanisms have broader application prospects. Our recent research had led to the design and development of a series of antioxidants and found a number of excellent antioxidants with scavenging ROS directly and indirectly. The most potent compound **33** not only showed protection of H₂O₂-induced

oxidative damage in PC12 cells through scavenging free radicals directly and activating NRF2 pathway at the same time, but also played protective and therapeutic roles against ischemia/reperfusion-related brain injury in animals. More importantly, compound **33** were superior to compounds (only free radical scavengers or NRF2 pathway stimulators) both *in vitro* and *in vivo*. Thus, our present study found a new candidate drug for cerebral ischemia-reperfusion injury treatment, clarified that the dual antioxidant mechanisms have a better prospect for drug development, and provided new ideas and tactics for drug research on stroke and other oxidative stress-induced diseases treatment.

5. Experimental

5.1. Chemistry

All chemical reagents were obtained commercially from Sigma–Aldrich (St Louis, MO, USA), Aladdin (Shanghai, China) and used without further purification unless otherwise noted. Reactions were monitored by thin-layer chromatography TLC using silica gel GF254, and the chromatograms were conducted on silica gel (200–300 mesh) and observed under UV light at 254 and 365 nm. Melting points (m.p.) are uncorrected and were measured in open capillary tubes on a Fisher–Johns melting apparatus. Mass spectra (MS) were recorded on an Agilent 1100 LC–MS (Agilent, Palo Alto, CA, USA). ^1H NMR and ^{13}C NMR spectra were obtained from 600 MHz spectrometer (Bruker Corporation, Switzerland). Chemical shifts are reported in δ units (ppm) relative to TMS as internal standard. Coupling constants (J) are expressed in Hz, and splitting patterns are described as follows: s=singlet; d=doublet; t=triplet; q=quartet; m=multiplet; dd=doublet of doublets; dt=doublet of triplets.

5.1.1. General procedure for the synthesis of chalcones

A mixture of the corresponding acetophenone (1 eq.) and the corresponding aldehyde (1 eq.) in anhydrous EtOH was stirred at room temperature for 5 min. Then NaOH or HCl (gas) was added into the solution to catalyze the reaction. The reaction mixture was stirred at room temperature until aldehyde was consumed (usually 12–24 h). Completion of the reaction was monitored by thin layer chromatography using ethyl acetate/hexanes as the solvent system. The reaction was quenched by pouring into 50 mL of stirring ice water. If the product precipitated out after quenching with cold water, it was filtered off and crystallized with hot ethanol. In other cases, the products were purified by using silica gel chromatography. Compounds **1–7**, **9–10**, **13**, **14**, **16**, **19–20**, **22**, **24**, **26**, **28**, **32**, **36**, **38** and **40** were published previously in the literature^{74–89}, and their spectral data are in the [Supporting Information](#). The spectral data of novel or unreported compounds are listed as follows.

(E)-3-(3,4-Dimethoxyphenyl)-1-(4-ethoxyphenyl)prop-2-en-1-one (8): Yellow power, 67.6% yield, m.p. 88.9–93.4 °C. ^1H NMR (DMSO- d_6) δ 8.165 (d, $J=9.0$ Hz, 2 H, H-2', H-6'), 7.839 (d, $J=15.5$ Hz, 1 H, H- β), 7.683 (d, $J=15.5$ Hz, 1 H, H- α), 7.544 (s, 1 H, H-2), 7.379 (d, $J=8.5$ Hz, 1 H, H-5), 7.069 (d, $J=9.0$ Hz, 2 H, H-3', H-5'), 7.022 (d, $J=8.5$ Hz, 1 H, H-6), 4.145 (q, $J=7.0$ Hz, 2 H, OCH₂-4'), 3.877 (s, 3 H, OCH₃-3), 3.824 (s, 3 H, OCH₃-4), 1.369 (t, $J=6.5$ Hz, 3 H, CH₃); ^{13}C NMR (DMSO- d_6) δ 187.25, 162.35, 151.13, 149.53, 143.53, 130.76 (2), 130.56, 127.67, 123.64, 119.62, 114.27 (2), 111.60, 110.82, 63.52,

55.74, 55.58, 14.45. HR-MS m/z 313.1436 [M + H]⁺, Calcd. for C₁₉H₂₀O₄: 312.1362.

(E)-3-(3,4-Dihydroxyphenyl)-1-(2-fluorophenyl)prop-2-en-1-one (11): Yellow green powder, 72.6% yield, m.p. 174.7–175.8 °C. ^1H NMR (Acetone- d_6) δ 8.581 (s, 1 H, OH-3), 8.255 (s, 1 H, OH-4), 7.760 (dd, $J=1.8$ Hz, $J=7.2$ Hz, 1 H, H-6'), 7.633–7.645 (m, 1 H, H-4'), 7.572 (dd, $J=1.2$ Hz, $J=15.6$ Hz, 1 H, H- β), 7.331–7.357 (m, 1 H, H-5'), 7.281–7.299 (m, 1 H, H-3'), 7.266 (d, $J=1.8$ Hz, 1 H, H-2), 7.213 (dd, $J=2.4$ Hz, $J=15.6$ Hz, 1 H, H- α), 7.142 (dd, $J=2.4$ Hz, $J=8.4$ Hz, 1 H, H-6), 6.904 (d, $J=7.8$ Hz, 1 H, H-5); ^{13}C NMR (DMSO- d_6) δ 188.55, 161.02, 159.02, 149.13, 145.70, 133.73, 130.30, 127.32, 125.71, 124.75, 122.54, 122.09, 116.58, 115.87, 114.97. HR-MS m/z 281.0593 [M + Na]⁺, Calcd. for C₁₅H₁₁FO₃: 258.0692.

(E)-1-(3,4-Dimethoxyphenyl)-3-(2-fluorophenyl)prop-2-en-1-one (12): Yellow powder, 67.4% yield, m.p. 90.5–92.4 °C. ^1H NMR (CDCl₃) δ 7.591 (d, $J=7.8$ Hz, 1 H, H-4'), 7.564–7.536 (m, 2 H, H-6', H-5'), 7.489 (d, $J=14.4$ Hz, 1 H, H- β), 7.403 (d, $J=1.8$ Hz, 1 H, H-6), 7.310–7.288 (m, 2 H, H-3', H-2), 7.188 (d, $J=16.2$ Hz, 1 H, H- α), 7.002 (d, $J=8.4$ Hz, 1 H, H-5), 3.809 (s, 6 H, OCH₃-3, OCH₃-4); ^{13}C NMR (DMSO- d_6) δ 187.93, 151.45, 149.04, 145.01, 137.81, 136.51, 130.29 (2), 128.77 (2), 127.40, 124.07, 119.28, 111.58, 110.93, 55.75, 55.59. HR-MS m/z 287.1071 [M + H]⁺, Calcd. for C₁₇H₁₅FO₃: 286.1005.

(E)-3-(3,4-Dihydroxyphenyl)-1-(4-fluorophenyl)prop-2-en-1-one (15): Yellow power, 78.8% yield, m.p. 224.4–226.0 °C. ^1H NMR (Acetone- d_6) δ 8.594 (s, 1 H, OH-3), 8.212 (t, $J=1.8$ Hz, 2 H, H-3', H-5'), 8.151 (s, 1 H, OH-4), 7.687 (d, $J=15.6$ Hz, 1 H, H- β), 7.624 (d, $J=15.6$ Hz, 1 H, H- α), 7.336 (d, $J=1.8$ Hz, 1 H, H-2), 7.298 (t, $J=8.7$ Hz, 2 H, H-2', H-6'), 7.210 (t, $J=8.4$ Hz, 1 H, H-6), 6.905 (d, $J=8.4$ Hz, 1 H, H-5); ^{13}C NMR (DMSO- d_6) δ 191.01, 152.10, 148.76, 145.85, 145.58, 145.11, 131.24, 131.16, 128.86, 126.21, 124.40, 122.23, 118.19, 115.50, 114.40. HR-MS m/z 281.0593 [M + Na]⁺, Calcd. for C₁₅H₁₁FO₃: 258.0692.

(E)-1-(3,4-Difluorophenyl)-3-(3,4-dihydroxyphenyl)prop-2-en-1-one (17): Yellow power, 77.9% yield, m.p. 234.9–236.4 °C. ^1H NMR (DMSO- d_6) δ 9.803 (s, 1 H, OH-3), 9.123 (s, 1 H, OH-4), 8.178–8.214 (m, 1 H, H-2'), 8.019–8.037 (m, 1 H, H-6'), 7.600–7.667 (m, 1 H, H-5'), 7.654 (d, $J=16.2$ Hz, 1 H, H- β), 7.628 (d, $J=16.2$ Hz, 1 H, H- α), 7.302 (d, $J=2.4$ Hz, 1 H, H-2), 7.218 (dd, $J=2.4$ Hz, $J=8.4$ Hz, 1 H, H-6), 6.819 (d, $J=8.4$ Hz, 1 H, H-5); ^{13}C NMR (DMSO- d_6) δ 186.38, 149.00, 145.80, 145.60, 126.16, 125.99, 125.93, 122.49, 117.92, 117.78, 117.74, 117.67, 117.53, 115.82, 115.70. HR-MS m/z 277.0682 [M + H]⁺, Calcd. for C₁₅H₁₀F₂O₃: 276.0598.

(E)-1-(3,4-Difluorophenyl)-3-(3,4-dimethoxyphenyl)prop-2-en-1-one (18): Yellow power, 75.0% yield, m.p. 118.6–120.4 °C. ^1H NMR (CDCl₃) δ 7.846–7.880 (m, 1 H, H-6'), 7.801–7.809 (m, 1 H, H-2'), 7.788 (d, $J=15.6$ Hz, 1 H, H- β), 7.309 (d, $J=15.6$ Hz, 1 H, H- α), 7.262–7.311 (m, 1 H, H-5'), 7.248 (dd, $J=1.8$ Hz, $J=8.4$ Hz, 1 H, H-6), 7.156 (d, $J=1.8$ Hz, 1 H, H-2), 6.913 (d, $J=7.8$ Hz, 1 H, H-5), 3.976 (s, 3 H, OCH₃-3), 3.945 (s, 3 H, OCH₃-4); ^{13}C NMR (DMSO- d_6) δ 182.45, 146.59, 144.15, 140.69, 122.32, 120.00, 119.94, 118.18, 113.59, 112.58, 112.44, 112.26, 112.12, 106.00, 105.04, 50.78 (2). HR-MS m/z 305.0982 [M + H]⁺, Calcd. for C₁₇H₁₄F₂O₃: 304.0911.

(E)-1-(3,5-Difluorophenyl)-3-(3,4-dihydroxyphenyl)prop-2-en-1-one (21): Yellow powder, 46.6% yield, m.p. 180.9–183.2 °C. ¹H NMR (Acetone-*d*₆) δ 7.729–7.764 (m, 3 H, H-β, H-2', H-6'), 7.672 (d, *J*=15.6 Hz, 1 H, H-α), 7.379 (d, *J*=1.8 Hz, 1 H, H-2), 7.305 (dd, *J*=2.4 Hz, *J*=8.4 Hz, 1 H, H-4'), 7.251 (dd, *J*=1.8 Hz, *J*=7.8 Hz, 1 H, H-6), 6.912 (d, *J*=7.8 Hz, 1 H, H-5); ¹³C NMR (DMSO-*d*₆) δ 191.00, 152.10, 149.17, 146.44, 145.86, 145.60, 128.86, 126.12, 124.39, 122.71, 117.68, 115.95, 115.70, 115.50, 114.40. HR-MS *m/z* 277.0682 [M + H]⁺, Calcd. for C₁₅H₈F₂O₃: 276.0598.

(E)-1-(3,4-Dihydroxyphenyl)-3-(4-methoxyphenyl)prop-2-en-1-one (23): Yellow crystal, 81.6% yield, m.p. 129.3–132.3 °C. ¹H NMR (CDCl₃) δ 7.800 (d, *J*=9.0 Hz, 2 H, H-2, H-6), 7.698 (d, *J*=15.0 Hz, 1 H, H-β), 7.614 (d, *J*=15.0 Hz, 1 H, H-α), 7.607 (dd, *J*=2.4 Hz, *J*=8.4 Hz, 1 H, H-6'), 7.499 (d, *J*=2.4 Hz, 1 H, H-2'), 7.002 (d, *J*=9.0 Hz, 2 H, H-3, H-5), 6.850 (d, *J*=8.4 Hz, 1 H, H-5'), 3.814 (s, 3 H, OCH₃-4); ¹³C NMR (DMSO-*d*₆) δ 187.14, 161.04, 150.66, 145.41, 142.32, 130.46 × 2, 129.84, 127.54, 121.87, 119.74, 115.40, 115.17, 114.36 (2), 55.32. HR-MS *m/z* 271.0995 [M + H]⁺, Calcd. for C₁₆H₁₄O₄: 270.0892.

(E)-1-(3,4-Dihydroxyphenyl)-3-(3-hydroxy-4-methoxyphenyl)prop-2-en-1-one (25): Yellow powder, 43.5% yield, m.p. 153.8–156.6 °C. ¹H NMR (DMSO-*d*₆) δ 7.601 (d, *J*=3.6 Hz, 1 H, H-β), 7.583 (t, *J*=5.4 Hz, 1 H, H-6'), 7.530 (d, *J*=15.6 Hz, 1 H, H-α), 7.491 (d, *J*=2.4 Hz, 1 H, H-2'), 7.273 (d, *J*=1.8 Hz, 1 H, H-2), 7.247 (dd, *J*=2.4 Hz, *J*=2.4 Hz, 1 H, H-6), 6.987 (d, *J*=6.4 Hz, 1 H, H-5'), 6.855 (d, *J*=7.8 Hz, 1 H, H-5), 3.835 (s, 3 H, OCH₃-4); ¹³C NMR (DMSO-*d*₆) δ 187.12, 150.70, 149.97, 146.65, 145.40, 142.82, 129.86, 127.85, 121.79, 121.56, 119.55, 115.31, 115.08, 114.62, 111.98, 55.66. HR-MS *m/z* 287.0914 [M + H]⁺, Calcd. for C₁₆H₁₄O₅: 286.0841.

(E)-1-(3,4-Dihydroxyphenyl)-3-(2,4-dimethoxyphenyl)prop-2-en-1-one (27): Yellow powder, 43.9% yield, m.p. 191.3–192.9 °C. ¹H NMR (DMSO-*d*₆) δ 7.928 (d, *J*=15.6 Hz, 1 H, H-β), 7.819 (d, *J*=15.6 Hz, 1 H, H-α), 7.626 (dd, *J*=3.0 Hz, *J*=2.4 Hz, 1 H, H-6), 7.505 (d, *J*=1.8 Hz, 1 H, H-6'), 7.494 (d, *J*=2.4 Hz, 1 H, H-2'), 7.044–6.997 (m, 2 H, H-5, H-5'), 6.859 (d, *J*=20.4 Hz, 1 H, H-3), 3.835 (s, 3 H, OCH₃-2), 3.790 (s, 3 H, OCH₃-4); ¹³C NMR (DMSO-*d*₆) δ 187.31, 162.70, 159.73, 150.50, 145.36, 137.27, 130.01, 129.95, 121.62, 119.35, 116.19, 115.30, 115.07, 106.23, 98.35, 55.78, 55.48. HR-MS *m/z* 301.1068 [M + H]⁺, Calcd. for C₁₇H₁₆O₅: 300.0998.

(E)-1-(3,4-Dihydroxyphenyl)-3-(2-methoxyphenyl)prop-2-en-1-one (29): Red-brown powder, 50.8% yield, m.p. 143.2–147.9 °C. ¹H NMR (CDCl₃) δ 8.107 (d, *J*=16.2 Hz, 1 H, H-β), 7.635 (d, *J*=16.2 Hz, 1 H, H-α), 7.773 (s, 1 H, H-2'), 7.591–7.635 (m, 2 H, H-5', H-6'), 7.381 (t, *J*=7.8 Hz, 1 H, H-4), 6.937–7.008 (m, 3 H, H-3, H-5, H-6'), 3.924 (s, 3 H, OCH₃-2); ¹³C NMR (DMSO-*d*₆) δ 187.38, 158.10, 150.81, 145.46, 137.06, 131.80, 129.72, 128.40, 123.22, 122.09, 121.91, 120.67, 115.33, 115.12, 111.74, 55.67. HR-MS *m/z* 271.0995 [M + H]⁺, Calcd. for C₁₆H₁₄O₄: 270.0892.

(E)-1-(3,4-Dimethoxyphenyl)-3-(2-methoxyphenyl)prop-2-en-1-one (30): Yellow powder, 58.9% yield, m.p. 53.9–55.0 °C. ¹H NMR (DMSO-*d*₆) δ 8.035 (d, *J*=15.6 Hz, 1 H, H-β), 7.989 (dd, *J*=1.8 Hz, *J*=1.8 Hz, 1 H, H-6'), 7.913–7.866 (m, 2 H, H-2', H-6), 7.599 (d, *J*=2.4 Hz, 1 H, H-3), 7.468–7.440 (m, 1 H, H-4), 7.118 (t, *J*=15.6 Hz, 2 H, H-5, H-5'), 7.044 (t, *J*=15.0 Hz, 1 H,

H-α), 3.907 (s, 3 H, OCH₃-3'), 3.879 (s, 3 H, OCH₃-4'), 3.866 (s, 3 H, OCH₃-2); ¹³C NMR (DMSO-*d*₆) δ 187.52, 158.16, 153.14, 148.85, 137.63, 131.84, 130.74, 128.32, 123.24, 123.08, 121.75, 120.56, 111.55, 110.75, 55.48 (3). HR-MS *m/z* 299.1212 [M + H]⁺, Calcd. for C₁₈H₁₈O₄: 298.1205.

(E)-1-(3,4-Dihydroxyphenyl)-3-(2,3-dimethoxyphenyl)prop-2-en-1-one (31): Brown yellow powder, 20.0% yield, m.p. 160.2–163.2 °C. ¹H NMR (DMSO-*d*₆) δ 9.960 (s, 1 H, OH-3'), 9.407 (s, 1 H, OH-4'), 7.905 (d, *J*=15.6 Hz, 1 H, H-β), 7.813 (d, *J*=16.0 Hz, 1 H, H-α), 7.624 (d, *J*=8.0 Hz, 1 H, H-6'), 7.572 (s, 1 H, H-6), 7.521 (s, 1 H, H-5), 7.139 (s, 2 H, H-2', H-5'), 6.878 (d, *J*=8.0 Hz, 1 H, H-4), 3.845 (s, 3 H, OCH₃-2), 3.798 (s, 3 H, OCH₃-3); ¹³C NMR (DMSO-*d*₆) δ 187.30, 152.77, 150.91, 148.10, 145.49, 136.50, 129.52, 128.44, 124.25, 123.10, 122.03, 119.15, 115.36, 115.12, 114.76, 60.86, 55.81. HR-MS *m/z* 301.1068 [M + H]⁺, Calcd. for C₁₇H₁₆O₅: 300.0998.

(E)-1-(3,4-Dihydroxyphenyl)-3-(2,5-dimethoxyphenyl)prop-2-en-1-one (33): Yellow powder, 56.8% yield, m.p. 95.4–97.9 °C. ¹H NMR (DMSO-*d*₆) δ 9.869 (s, 1 H, OH-3'), 9.320 (s, 1 H, OH-4'), 7.926 (d, *J*=19.2 Hz, 1 H, H-β), 7.803 (d, *J*=19.2 Hz, 1 H, H-α), 7.615 (d, *J*=9.6 Hz, 1 H, H-6'), 7.495 (d, *J*=19.2 Hz, 2 H, H-2', H-5'), 7.029 (d, *J*=8.4 Hz, 2 H, H-3, H-6), 6.872 (d, *J*=9.0 Hz, 1 H, H-4), 3.845 (s, 3 H, OCH₃-2), 3.799 (s, 3 H, OCH₃-5); ¹³C NMR (DMSO-*d*₆) δ 187.36, 153.26, 152.56, 150.84, 145.45, 136.79, 129.70, 123.79, 122.28, 122.04, 117.63, 115.38, 115.07, 113.04, 112.62, 56.15, 55.67. HR-MS *m/z* 301.1068 [M + H]⁺, Calcd. for C₁₇H₁₆O₅: 300.0998.

(E)-3-(2,5-Dimethoxyphenyl)-1-(3,4-dimethoxyphenyl)prop-2-en-1-one (34): Yellow powder, 74.3% yield, m.p. 72.5–73.4 °C. ¹H NMR (CDCl₃) δ 8.066 (d, *J*=15.5 Hz, 1 H, H-β), 7.680 (d, *J*=8.0 Hz, 1 H, H-6'), 7.607 (d, *J*=18.0 Hz, 2 H, H-2', H-α), 7.178 (s, 1 H, H-6), 6.938 (d, *J*=7.5 Hz, 2 H, H-3, H-4), 6.884 (d, *J*=8.5 Hz, 1 H, H-5'), 3.974 (s, 6 H, OCH₃-3', OCH₃-4'), 3.878 (s, 3 H, OCH₃-2), 3.826 (s, 3 H, OCH₃-5); ¹³C NMR (CDCl₃) δ 189.25, 153.59, 153.30, 153.14, 149.22, 139.33, 131.61, 124.86, 123.00 (2), 116.86, 113.97, 112.53, 111.03, 110.06, 56.16, 56.07, 56.05, 55.87. HR-MS *m/z* 329.1389 [M + H]⁺, Calcd. for C₁₉H₂₀O₅: 328.1311.

(E)-3-(4-Chlorophenyl)-1-(3,4-dihydroxyphenyl)prop-2-en-1-one (35): Light powder, 34.8% yield, m.p. 216.4–217.8 °C. ¹H NMR (DMSO-*d*₆) δ 9.980 (s, 1 H, OH-3'), 9.386 (s, 1 H, OH-4'), 7.906 (s, 1 H, H-β), 7.886 (t, *J*=15.0 Hz, 2 H, H-6, H-2), 7.666–7.623 (m, 2 H, H-2', H-6'), 7.523 (d, *J*=2.4 Hz, 2 H, H-3, H-5), 7.507 (s, 1 H, H-α), 6.869 (d, *J*=8.4 Hz, 1 H, H-5'); ¹³C NMR (DMSO-*d*₆) δ 188.55, 161.02, 159.02, 149.13, 145.70, 133.73, 130.30, 127.32, 125.71, 124.75, 122.54, 122.09, 116.58, 115.87, 114.97. HR-MS *m/z* 275.0502 [M + H]⁺, Calcd. for C₁₅H₁₁ClO₃: 274.0397.

(E)-3-(3,4-Dichlorophenyl)-1-(3,4-dihydroxyphenyl)prop-2-en-1-one (37): Dark purple syrupy, 49.2% yield. ¹H-NMR (DMSO-*d*₆) δ 9.808 (s, 1 H, OH-3'), 9.122 (s, 1 H, OH-4'), 8.196 (t, *J*=9.0 Hz, 1 H, H-β), 8.025 (s, 1 H, H-2'), 7.643–7.591 (m, 3 H, H-α, H-6', H-6), 7.305 (s, 1 H, H-2), 7.218 (d, *J*=9.5 Hz, 1 H, H-5'), 6.956 (d, *J*=8.0 Hz, 1 H, H-5). ¹³C NMR (DMSO-*d*₆) δ 186.94, 151.16, 145.53, 139.55, 135.85, 132.29, 131.76, 130.88, 129.91, 129.39, 128.82, 124.36, 122.43, 115.46, 115.04. HR-MS *m/z* 308.9991 [M + H]⁺, Calcd. for C₁₅H₁₀Cl₂O₃: 308.0007.

(E)-1-(3,4-Dihydroxyphenyl)-3-(3,4,5-trimethoxyphenyl)prop-2-en-1-one (39): Yellow powder, 56.4% yield, m.p. 118.9–121.0 °C. ¹H NMR (CDCl₃) δ 9.944 (s, 1 H, OH-3'), 9.370 (s, 1 H, OH-4'), 7.814 (d, *J*=12.0 Hz, 1 H, H-β), 7.671 (dd, *J*=2.4 Hz, *J*=2.4 Hz, 1 H, H-6'), 7.609 (d, *J*=15.0 Hz, 1 H, H-α), 7.533 (d, *J*=2.4 Hz, 1 H, H-2'), 7.195 (s, 2 H, H-2, H-6), 6.882 (d, *J*=7.8 Hz, 1 H, H-5'), 3.865 (s, 6 H, OCH₃-3, OCH₃-5), 3.712 (s, 3 H, OCH₃-4); ¹³C NMR (DMSO-*d*₆) δ 187.21, 153.09 (2), 150.82, 145.45, 142.85, 139.51, 130.48, 129.72, 122.13, 121.43, 115.43, 115.00, 106.30 (2), 60.10, 56.11 (2). HR-MS *m/z* 353.0999 [M + Na]⁺, Calcd. for C₁₈H₁₈O₆: 330.1103.

(E)-1-(3,4-Dihydroxyphenyl)-3-(3,4-dimethoxyphenyl)prop-2-en-1-one (41): Yellow powder, 64.3% yield, m.p. 109.5–111.0 °C. ¹H NMR (CDCl₃) δ 7.737 (d, *J*=15.6 Hz, 1 H, H-β), 7.648 (dd, *J*=1.8 Hz, *J*=1.8 Hz, 1 H, H-6'), 7.608 (d, *J*=15.6 Hz, 1 H, H-α), 7.519 (d, *J*=1.8 Hz, 1 H, H-2'), 7.508 (d, *J*=1.8 Hz, 1 H, H-2), 7.337 (dd, *J*=1.8 Hz, *J*=1.8 Hz, 1 H, H-6), 7.015 (d, *J*=8.4 Hz, 1 H, H-5'), 6.867 (d, *J*=8.4 Hz, 1 H, H-5), 3.863 (s, 3 H, OCH₃-3), 3.817 (s, 3 H, OCH₃-4); ¹³C NMR (DMSO-*d*₆) δ 187.36, 153.26, 152.56, 150.84, 145.45, 136.79, 129.70, 123.79, 122.28, 122.04, 117.63, 115.38, 115.07, 113.04, 112.62, 56.15, 55.67. HR-MS *m/z* 301.1068 [M + H]⁺, Calcd. for C₁₇H₁₆O₅: 300.0998.

5.2. Pharmacology

5.2.1. DPPH assay

The DPPH assay measured hydrogen atom (or one electron) donating activity and hence provided an evaluation of antioxidant activity due to free radical scavenging⁹⁰. The test was prepared as described previously^{44,91}.

5.2.2. Cell culture

PC12 cells, rat pheochromocytoma cell lines, were obtained from the Cell Storage Center of Wuhan University (Wuhan, China). Cells were grown in 1 × DMEM supplemented with 10% fetal bovine serum (FBS), containing 100 U/mL penicillin and 100 U/mL streptomycin, and incubated at 37 °C with 5% CO₂.

5.2.3. MTT assay

3-[4,5-Dimethylthiazol-2-yl]-2,5-diphenyltetrazolium bromide, thiazolyl blue (MTT) assay was used to measure cell viability. Briefly, cells were seeded in 96-well plates and cultured for 24 h. After appropriate treatments, the cells were incubated with 20 μL MTT (0.5 mg/mL). Following incubation at 37 °C for 4 h, media were aspirated from each well and DMSO (120 μL) was added. The absorbance was measured at λ=490 nm using a Microplate Reader (Bio-Rad, USA). Assays were repeated at least three times.

5.2.4. Lipid peroxidation assay

Levels of Malondialdehyde (MDA) were determined using the assay kit (Nanjing Jiancheng Bioengineering Institute, Nanjing, China) according to the manufacturer's instruction. At the end of the drug treatment, supernatants in the cells were collected through centrifugation. Supernatants were mixed with TBA (0.37%) solution and then boiled for 15 min at 100 °C. The samples were rapidly cooled to room temperature, and were determined with a microplate reader at a wavelength of 532 nm.

5.2.5. Detection of reactive oxygen species

Intracellular ROS generation was assessed with dichlorodihydrofluorescein diacetate (DCFH-DA, Beyotime Biotechnology, Shanghai, China). Cells were stained with 1 μL DCFH-DA (10 μmol/L) for 30 min at 37 °C in the dark. Cells were trypsinized, harvested, washed three times with PBS, resuspended in PBS and then analyzed by flow cytometry (Becton Dickinson, USA).

5.2.6. Immunofluorescence

PC12 cells were fixed with 4% paraformaldehyde for 20 min at room temperature and washed three times with PBS. The cells were permeabilized in 0.1% TritonX-100 (Sigma-Aldrich St. Louis, MO, USA) for 15 min and blocked in 1% BSA for 1 h at room temperature. After being washed, the cells were incubated with a 1:200 dilution of primary NRF2 antibody (sc-13032, Santa Cruz Biotechnology, USA, 1:200) at 4 °C overnight and incubated with appropriate secondary antibody (sc-13032, goat anti-rabbit IgG-PE, Santa Cruz Biotechnology, USA, 1:300) for 1 h at room temperature. Cell nuclei were stained with DAPI. The images were acquired with the fluorescence microscope (Nikon, Japan).

5.2.7. Real-time PCR analyses

After various treatments, the cells were collected and total RNA was extracted. Then, reverse transcription (RT) was performed with M-MLV Reverse Transcriptase (Thermo Fisher Scientific, MA, USA) as following: 65 °C for 5 min for the reverse transcription. And the real-time PCR assay was performed at 37 °C for 50 min and 70 °C for 15 min for the PCR reaction, with 40 cycles. Relative levels of mRNA were analysed by the following primers.

For *mHO-1*: 5'-GCCTGCTAGCCTGGTCAAG-3'; 5'-AGCGGTGTCTGGGATGA ACTA-3'.

For *mGCLC*: 5'-GTCCTCAGGTGA CATTCCAAGC-3'; 5'-TGTTCTTCAGG GGCTCCAGTC-3'.

For *mGADPH*: 5'-AAGCTGGTCATCA ACGGGAAAC-3'; 5'-GAAGACGCCAG TAGACTCCACG-3'.

Relative mRNA expression values were calculated by the^{-ΔΔCt} method⁹².

5.2.8. Western blot analysis

PC12 cells were incubated in 6-well plates at a density of 3 × 10⁵ and incubated for 24–48 h at 37 °C. After suitable treatments, the cells were collected and lysed with ice-cold RIPA lysis buffer. Equal amounts of protein samples (80 μg) were separated on a 10% SDS-PAGE gel and transferred electrophoretically onto nitrocellulose membrane. Subsequently, the membranes were blocked with 5% skim milk and incubated overnight at 4 °C with primary antibody: anti-HO-1 (sc-10789, Santa Cruz Biotechnology, 1:300), anti-GCLC (ab-80841, abcam Biotechnology, 1:600), anti-GADPH (sc-47724, Santa Cruz Biotechnology, 1:1000), anti-β-actin (AP0060, Bioworld Technology, 1:3000). After being washed three times with 1 × TBST, the membrane was incubated with anti-rabbit IgG for 1 h at room temperature. Proteins were visualized by exposure in a ChemiDoc XRS+system (Bio-Rad, Hercules, CA, USA). Band density was quantified by Image J software (National Institute of Health, Bethesda, MD, USA).

5.2.9. Materials and animals

2,3,5-Triphenyltetrazolium (TTC) was purchased from Sigma (St. Louis, MO, USA). Chloral hydrate was purchased from Sinopharm Chemical Reagent Co., Ltd. (Shanghai, China). **33** and edaravone (ED)

was dissolved in a solvent (Cremophor:PBS at 3:97) for the intraperitoneal injection. **33/21/1b**-nanoparticles were prepared for the intracerebroventricular injection. The **33/21/1b**-loaded nanoparticles were prepared as described previously⁹³. All animals were obtained from the Shanghai Slaccas Lab Animal Co., Ltd. All animal experiments and care were performed according to the Guide for the Care and Use of Laboratory Animals (National Academy Press, Washington D.C., USA, 1996). Animals were fed with a standard laboratory diet, and were housed in a temperature-controlled room (24 °C) and illuminated for 12 h daily (lights on from 5 a.m. to 5 p.m.).

5.2.10. BCAO-induced cerebral ischemia/reperfusion injury in mice

This ischemia/reperfusion model was carried out as described by Himori et al.⁹⁴ with slight modifications. Briefly, male 8-week-old C57BL/6 mice were anaesthetized using 4% of chloral hydrate (0.1 mL/10 g; i.p.). A midline incision was made in the neck and the left and right carotid arteries were exposed. A loose silk ligature for occlusion (ischemia) was placed around both carotid arteries. Occlusion was maintained for 20 min, and this was followed by reperfusion for 24 h. In sham-operated animals, the arteries were exposed but not occluded. All mice were injected intraperitoneally 3 or 6 h after bilateral common carotid artery occlusion (BCAO).

5.2.11. Spontaneous locomotor activity test

After 24 h of reperfusion, the animals were placed in an open square chamber (40 cm³ box) equipped with horizontal and vertical infrared photo beams. Then, its behaviors were recorded for 5 min using the DigBehv software (DigBehav, Jiliang Co., Ltd., Shanghai, China). The locomotor activity was evaluated by measuring the total distance traveled in the apparatus.

5.2.12. MCAO-induced transient focal cerebral ischemia in rats

Male Sprague–Dawley rats (250–280 g) were used in this study. Rats have no interference factors such as infection and inflammation, and were used as the object of middle cerebral artery occlusion (MCAO) method. Firstly, rats were anesthetized with 10% of chloral hydrate (0.33–0.35 mL/100 kg; i.p.), and then placed them in the supine position. Secondly, after disinfection with iodine, the skin was cut. The common carotid artery (CCA), external carotid artery (ECA) and internal carotid artery (ICA) were separated. Thirdly, the CCA and the ECA was ligated while the ICA was closed with an artery clamp temporarily. Then tiny incisions were made at the distance of 4 mm from the branch of CCA. The MCAO model was established by inserting thread through CCA into the anterior cerebral artery. The sham-operated group was treated with the same operation without ischemia-reperfusion.

5.2.13. Neurological deficit score and TTC staining

Neurological score was assessed 24 or 72 h after MCAO in rats. Five types of motor neurological findings are as follows. 0: no obvious deficit; 1: difficult to extend the lateral forelimb fully; 2: cannot extend the lateral forelimbs; 3: circling to the contralateral side; 4: difficult or impossible to move or roll spontaneously. TTC staining was performed to determine the infarct area. Firstly, the brain of the rat was taken out in time and placed in the refrigerator at –20 °C for 20 min. Secondly, the brain was cut into five slices with 2 mm thickness and placed in TTC staining (Sigma–Aldrich, USA) at 37 °C for 30

min. The TTC-stained brain slices were taken pictures with the camera, and then the Image-Pro plus was used to handle the infarct area.

5.2.14. Statistical analysis

Data were presented as means ± SEM. The statistical differences between groups were determined by the Student's *t*-test or one-way analysis of variance for multiple comparisons in GraphPad Pro (GraphPad, San Diego, CA, USA). Differences were considered to be significant at *P* < 0.05.

Acknowledgments

The work was supported by Zhejiang Province Natural Science Funding of China (Nos. LQ18H280008, Y19B020043, and LY17H160059, China), the National Natural Science Foundation of China (No. 81803580, China), University Students in Zhejiang Science and Technology Innovation Projects (No. 2018R413004, China), National Undergraduate Training Programs for Innovation and Entrepreneurship (No. 201810343025, China) and Granted by the Opening Project of Zhejiang Provincial Top Key Discipline of Pharmaceutical Sciences.

Appendix A. Supporting information

Supplementary data associated with this article can be found in the online version at <https://doi.org/10.1016/j.apsb.2019.01.003>.

References

1. Flynn RW, MacWalter RS, Doney AS. The cost of cerebral ischaemia. *Neuropharmacology* 2008;**55**:250–6.
2. Durai Pandian J, Padma V, Vijaya P, Sylaja PN, Murthy JM. Stroke and thrombolysis in developing countries. *Int J Stroke* 2007;**2**:17–26.
3. Uchino K. Presenting to primary stroke centers or comprehensive stroke centers for thrombolysis. *JAMA Neurol* 2017;**74**:1269.
4. Wu J, Ling J, Wang X, Li T, Liu J, Lai Y, et al. Discovery of a potential anti-ischemic stroke agent: 3-pentylbenzo[*c*]thiophen-1(3*H*)-one. *J Med Chem* 2012;**55**:7173–81.
5. Candelario-Jalil E. Injury and repair mechanisms in ischemic stroke: considerations for the development of novel neurotherapeutics. *Curr Opin Investig Drugs* 2009;**10**:644–54.
6. Yen TL, Hsu CK, Lu WJ, Hsieh CY, Hsiao G, Chou DS, et al. Neuroprotective effects of xanthohumol, a prenylated flavonoid from hops (*Humulus lupulus*), in ischemic stroke of rats. *J Agric Food Chem* 2012;**60**:1937–44.
7. Eltzschig HK, Eckle T. Ischemia and reperfusion—from mechanism to translation. *Nat Med* 2011;**17**:1391–401.
8. Pantazi E, Bejaoui M, Folch-Puy E, Adam R, Roselló-Catafau J. Advances in treatment strategies for ischemia reperfusion injury. *Expert Opin Pharmacother* 2016;**17**:169–79.
9. Trippier PC, Jansen Labby K, Hawker DD, Mataka JJ, Silverman RB. Target- and mechanism-based therapeutics for neurodegenerative diseases: strength in numbers. *J Med Chem* 2013;**56**:3121–47.
10. Pérez-González A, Galano A. OH radical scavenging activity of Edaravone: mechanism and kinetics. *J Phys Chem B* 2011;**115**:1306–14.
11. Dinkova-Kostova AT, Talalay P. Direct and indirect antioxidant properties of inducers of cytoprotective proteins. *Mol Nutr Food Res* 2008;**52**:S128–38.
12. Jung KA, Kwak MK. The NRF2 system as a potential target for the development of indirect antioxidants. *Molecules* 2010;**15**:7266–91.

13. Magesh S, Chen Y, Hu L. Small molecule modulators of KEAP1-NRF2-ARE pathway as potential preventive and therapeutic agents. *Med Res Rev* 2012;**32**:687–726.
14. Guo Z. The modification of natural products for medical use. *Acta Pharm Sin B* 2017;**7**:119–36.
15. Rigano D, Sirignano C, Tagliatalata-Scafati O. The potential of natural products for targeting PPAR α . *Acta Pharm Sin B* 2017;**7**:427–38.
16. Wu JZ, Xi YY, Huang LL, Li G, Mao QQ, Fang CY, et al. A steroid-type antioxidant targeting the KEAP1/NRF2/ARE signaling pathway from the soft coral *Dendronephthya gigantea*. *J Nat Prod* 2018;**81**:2567–75.
17. Dimmock JR, Elias DW, Beazely MA, Kandepu NM. Bioactivities of chalcones. *Curr Med Chem* 1999;**6**:1125–49.
18. Niu H, Wang W, Li J, Lei Y, Zhao Y, Yang W, et al. A novel structural class of coumarin-chalcone fibrates as PPAR α / γ agonists with potent antioxidant activities: design, synthesis, biological evaluation and molecular docking studies. *Eur J Med Chem* 2017;**138**:212–20.
19. Cheng JH, Hung CF, Yang SC, Wang JP, Won SJ, Lin CN. Synthesis and cytotoxic, anti-inflammatory, and anti-oxidant activities of 2',5'-dialkoxychalcones as cancer chemopreventive agents. *Bioorg Med Chem* 2008;**16**:7270–6.
20. El Sayed Aly MR, Abd El Razeq Fodah HH, Saleh SY. Antiobesity, antioxidant and cytotoxicity activities of newly synthesized chalcone derivatives and their metal complexes. *Eur J Med Chem* 2014;**76**:517–30.
21. Wu JZ, Wang C, Cai YP, Peng J, Liang DL, Zhao YJ, et al. Synthesis and crystal structure of chalcones as well as on cytotoxicity and antibacterial properties. *Med Chem Res* 2012;**21**:444–52.
22. Lorenzo P, Alvarez R, Ortiz MA, Alvarez S, Piedrafita FJ, De Lera AR. Inhibition of I κ B kinase- β and anticancer activities of novel chalcone adamantyl arotinoids. *J Med Chem* 2008;**51**:5431–40.
23. Zhu M, Wang JB, Xie JW, Chen LP, Wei XY, Jiang X, et al. Design, synthesis, and evaluation of chalcone analogues incorporate α,β -unsaturated ketone functionality as anti-lung cancer agents via evoking ROS to induce pyroptosis. *Eur J Med Chem* 2018;**157**:1395–405.
24. Tuncel S, Fournier-dit-Chabert J, Albrieux F, Ahsen V, Ducki S, Dumoulin F. Towards dual photodynamic and antiangiogenic agents: design and synthesis of a phthalocyanine-chalcone conjugate. *Org Biomol Chem* 2012;**10**:1154–7.
25. Zhang YL, Wu JZ, Ying SL, Chen GZ, Wu BB, Xu TT, et al. Discovery of new MD2 inhibitor from chalcone derivatives with anti-inflammatory effects in LPS-induced acute lung injury. *Sci Rep* 2016;**6**:25130–42.
26. Wu J, Li J, Cai Y, Pan Y, Ye F, Zhang Y, et al. Evaluation and discovery of novel synthetic chalcone derivatives as anti-inflammatory agents. *J Med Chem* 2011;**54**:8110–23.
27. Menezes JC, Kamat SP, Cavaleiro JA, Gaspar A, Garrido J, Borges F. Synthesis and antioxidant activity of long chain alkyl hydroxycinnamates. *Eur J Med Chem* 2011;**46**:773–7.
28. Gaspar A, Martins M, Silva P, Garrido EM, Garrido J, Firuzi O, et al. Dietary phenolic acids and derivatives. Evaluation of the antioxidant activity of sinapic acid and its alkyl esters. *J Agric Food Chem* 2010;**58**:11273–80.
29. Cos P, Rajan P, Vedernikova I, Calomme M, Pieters L, Vlietinck AJ, et al. *In vitro* antioxidant profile of phenolic acid derivatives. *Free Radic Res* 2002;**36**:711–6.
30. Teixeira J, Cagide F, Benfeito S, Soares P, Garrido J, Baldeiras I, et al. Development of a mitochondriotropic antioxidant based on caffeic acid: proof of concept on cellular and mitochondrial oxidative stress models. *J Med Chem* 2017;**60**:7084–98.
31. Kumar V, Kumar S, Hassan M, Wu H, Thimmulappa RK, Kumar A, et al. Novel chalcone derivatives as potent NRF2 activators in mice and human lung epithelial cells. *J Med Chem* 2011;**54**:4147–59.
32. Kozłowski D, Trouillas P, Calliste C, Marsal P, Lazzaroni R, Duroux JL. Density functional theory study of the conformational, electronic, and antioxidant properties of natural chalcones. *J Phys Chem A* 2007;**111**:1138–45.
33. Rao YK, Fang SH, Tzeng YM. Synthesis and biological evaluation of 3',4',5'-trimethoxychalcone analogues as inhibitors of nitric oxide production and tumor cell proliferation. *Bioorg Med Chem* 2009;**17**:7909–14.
34. Meng CQ, Ni L, Worsencroft KJ, Ye Z, Weingarten MD, Simpson JE, et al. Carboxylated, heteroaryl-substituted chalcones as inhibitors of vascular cell adhesion molecule-1 expression for use in chronic inflammatory diseases. *J Med Chem* 2007;**50**:1304–15.
35. Bandgar BP, Patil SA, Korbad BL, Nile SH, Khobragade CN. Synthesis and biological evaluation of β -chloro vinyl chalcones as inhibitors of TNF- α and IL-6 with antimicrobial activity. *Eur J Med Chem* 2010;**45**:2629–33.
36. Ning X, Guo Y, Wang X, Ma X, Tian C, Shi X, et al. Design, synthesis, and biological evaluation of (*E*)-3,4-dihydroxystyryl aralkyl sulfones and sulfoxides as novel multifunctional neuroprotective agents. *J Med Chem* 2014;**57**:4302–12.
37. Talalay P, Dinkova-Kostova AT, Holtzclaw WD. Importance of phase 2 gene regulation in protection against electrophile and reactive oxygen toxicity and carcinogenesis. *Adv Enzyme Regul* 2003;**43**:121–34.
38. Yao J, Zhang B, Ge C, Peng S, Fang J. Xanthohumol, a polyphenol chalcone present in hops, activating NRF2 enzymes to confer protection against oxidative damage in PC12 cells. *J Agric Food Chem* 2015;**63**:1521–31.
39. Peng S, Zhang B, Meng X, Yao J, Fang J. Synthesis of piperlongumine analogues and discovery of nuclear factor erythroid 2-related factor 2 (NRF2) activators as potential neuroprotective agents. *J Med Chem* 2015;**58**:5242–55.
40. Peng S, Hou Y, Yao J, Fang J. Activation of NRF2-driven antioxidant enzymes by cardamonin confers neuroprotection of PC12 cells against oxidative damage. *Food Funct* 2017;**8**:997–1007.
41. Olatunji OJ, Chen H, Zhou Y. Neuroprotective effect of *trans-N*-caffeoyltyramine from *Lycium chinese* against H₂O₂ induced cytotoxicity in PC12 cells by attenuating oxidative stress. *Biomed Pharmacother* 2017;**93**:895–902.
42. Cao GS, Li SX, Wang Y, Xu YQ, Lv YN, Kou JP, et al. A combination of four effective components derived from Sheng-mai san attenuates hydrogen peroxide-induced injury in PC12 cells through inhibiting Akt and MAPK signaling pathways. *Chin J Nat Med* 2016;**14**:508–17.
43. Wu JZ, Cheng CC, Shen LL, Wang ZK, Wu SB, Li WL, et al. Synthetic chalcones with potent antioxidant ability on H₂O₂-induced apoptosis in PC12 cells. *Int J Mol Sci* 2014;**15**:18525–39.
44. Huang L, Wang J, Chen L, Zhu M, Wu S, Chu S, et al. Design, synthesis, and evaluation of NDGA analogues as potential anti-ischemic stroke agents. *Eur J Med Chem* 2018;**143**:1165–73.
45. Jiao ZZ, Yue S, Sun HX, Jin TY, Wang HN, Zhu RX, et al. Indoline amide glucosides from *Portulaca oleracea*: isolation, structure, and DPPH radical scavenging activity. *J Nat Prod* 2015;**78**:2588–97.
46. Chen J, Zeng L, Xia T, Li S, Yan T, Wu S, et al. Toward a biomarker of oxidative stress: a fluorescent probe for exogenous and endogenous malondialdehyde in living cells. *Anal Chem* 2015;**87**:8052–6.
47. Wu J, Ren J, Yao S, Wang J, Huang L, Zhou P, et al. Novel antioxidants' synthesis and their anti-oxidative activity through activating NRF2 signaling pathway. *Bioorg Med Chem Lett* 2017;**27**:1616–9.
48. Wang X, Wang L, Li T, Huang Z, Lai Y, Ji H, et al. Novel hybrids of optically active ring-opened 3-*n*-butylphthalide derivative and isosorbide as potential anti-ischemic stroke agents. *J Med Chem* 2013;**56**:3078–89.
49. Liu Y, Ai K, Ji X, Askhatova D, Du R, Lu L, et al. Comprehensive insights into the multi-antioxidative mechanisms of melanin nanoparticles and their application to protect brain from injury in ischemic stroke. *J Am Chem Soc* 2017;**139**:856–62.
50. The IST-3 Collaborative Group. The benefits and harms of intravenous thrombolysis with recombinant tissue plasminogen activator within 6 h

- of acute ischaemic stroke (the third international stroke trial [IST-3]): a randomised controlled trial. *Lancet* 2012;**379**:2352–63.
51. Evenson KR, Rosamond WD, Morris DL. Prehospital and in-hospital delays in acute stroke care. *Neuroepidemiology* 2001;**20**:65–76.
 52. Chang C, Zhao Y, Song G, She K. Resveratrol protects hippocampal neurons against cerebral ischemia-reperfusion injury via modulating JAK/ERK/STAT signaling pathway in rats. *J Neuroimmunol* 2018;**315**:9–14.
 53. Farías JG, Molina VM, Carrasco RA, Zepeda AB, Figueroa E, Letelier P, et al. Antioxidant therapeutic strategies for cardiovascular conditions associated with oxidative stress. *Nutrients* 2017;**9**:966–88.
 54. Patel RP, Lang JD, Smith AB, Crawford JH. Redox therapeutics in hepatic ischemia reperfusion injury. *World J Hepatol* 2014;**6**:1–8.
 55. Margail I, Plotkine M, Lerouet D. Antioxidant strategies in the treatment of stroke. *Free Radic Biol Med* 2005;**39**:429–43.
 56. Dennis JM, Witting PK. Protective role for antioxidants in acute kidney disease. *Nutrients* 2017;**9**:718.
 57. Panizo N, Rubio-Navarro A, Amaro-Villalobos JM, Egido J, Moreno JA. Molecular mechanisms and novel therapeutic approaches to rhabdomyolysis-induced acute kidney injury. *Kidney Blood Press Res* 2015;**40**:520–32.
 58. Carroll JE, Howard EF, Hess DC, Wakade CG, Chen Q, Cheng C. Nuclear factor- κ B activation during cerebral reperfusion: effect of attenuation with *N*-acetylcysteine treatment. *Mol Brain Res* 1998;**56**:186–91.
 59. Shah ZA, Li RC, Thimmulappa RK, Kensler TW, Yamamoto M, Biswal S, et al. Role of reactive oxygen species in modulation of NRF2 following ischemic reperfusion injury. *Neuroscience* 2007;**147**:53–9.
 60. Shih AY, Li P, Murphy TH. A small-molecule-inducible NRF2-mediated antioxidant response provides effective prophylaxis against cerebral ischemia *in vivo*. *J Neurosci* 2005;**25**:10321–35.
 61. Sun J, Ren X, Simpkins JW. Sequential upregulation of superoxide dismutase 2 and heme oxygenase 1 by *tert*-butylhydroquinone protects mitochondria during oxidative stress. *Mol Pharm* 2015;**88**:437–49.
 62. Joko S, Watanabe M, Fuda H, Takeda S, Furukawa T, Hui SP, et al. Comparison of chemical structures and cytoprotection abilities between direct and indirect antioxidants. *J Funct Foods* 2017;**35**:245–55.
 63. Manev H, Uz T, Kharlamov A, Joo JY. Increased brain damage after stroke or excitotoxic seizures in melatonin-deficient rats. *FASEB J* 1996;**10**:1546–51.
 64. Ren J, Fan C, Chen N, Huang J, Yang Q. Resveratrol pretreatment attenuates cerebral ischemic injury by upregulating expression of transcription factor NRF2 and HO-1 in rats. *Neurochem Res* 2011;**36**:2352–62.
 65. Yang C, Zhang X, Fan H, Liu Y. Curcumin upregulates transcription factor NRF2, HO-1 expression and protects rat brains against focal ischemia. *Brain Res* 2009;**1282**:133–41.
 66. Jeon KH, Lee E, Jun KY, Eom JE, Kwak SY, Na Y, et al. Neuroprotective effect of synthetic chalcone derivatives as competitive dual inhibitors against mu-calpain and cathepsin B through the downregulation of tau phosphorylation and insoluble A β peptide formation. *Eur J Med Chem* 2016;**121**:433–44.
 67. Padmavathi G, Roy NK, Bordoloi D, Arfuso F, Mishra S, Sethi G, et al. Butein in health and disease: a comprehensive review. *Phyto-medicine* 2017;**25**:118–27.
 68. Lee MJ, Lee HS, Kim H, Yi HS, Park SD, Moon HI, et al. Antioxidant properties of benzylchroman derivatives from *Caesalpinia sappan* L. against oxidative stress evaluated *in vitro*. *J Enzym Inhib Med Chem* 2010;**25**:608–14.
 69. Wang W, Chen W, Yang YS, Liu TX, Yang HY, Xin ZH. New phenolic compounds from *Coreopsis tinctoria* Nutt. and their antioxidant and angiotensin I-converting enzyme inhibitory activities. *J Agric Food Chem* 2015;**63**:200–7.
 70. Chiruta C, Schubert D, Dargusch R, Maher P. Chemical modification of the multitarget neuroprotective compound fisetin. *J Med Chem* 2012;**55**:378–89.
 71. Dziedzic SZ, Hudson BJF. Polyhydroxy chalcones and flavanones as antioxidants for edible oils. *Food Chem* 1983;**12**:205–12.
 72. Benayahoum A, Amira-Guebailia H, Houache OA. DFT method for the study of the antioxidant action mechanism of resveratrol derivatives. *J Mol Model* 2013;**19**:2285–98.
 73. Foti C, Piattelli M, Baratta MT, Ruberto G. Flavonoids, coumarins, and cinnamic acids as antioxidants in a micellar system. Structure–activity relationship. *J Agric Food Chem* 1996;**44**:497–501.
 74. Sogawa S, Nihro Y, Ueda H, Izumi A, Miki T, Matsumoto H, et al. 3,4-Dihydroxychalcones as potent 5-lipoxygenase and cyclooxygenase inhibitors. *J Med Chem* 1993;**36**:3904–9.
 75. Bodiwala HS, Sabde S, Gupta P, Mukherjee R, Kumar R, Garg P, et al. Design and synthesis of caffeoyl-anilides as portmanteau inhibitors of HIV-1 integrase and CCR5. *Bioorg Med Chem* 2011;**19**:1256–63.
 76. Sharma N, Joshi YC. Synthesis of substituted chalcones under solvent-free microwave irradiation conditions and their antimicrobial evaluation. *Int J Pharm Pharm Sci* 2012;**4**:436–9.
 77. Bai XG, Xu CL, Zhao SS, He HW, Wang YC, Wang JX. Synthesis and cytotoxic evaluation of alkoxyated chalcones. *Molecules* 2014;**19**:17256–78.
 78. Wu JZ, Li WL, Chen LZ, Chu SH, Zhao CG, Wei TY, et al. Synthesis, crystal structure, antioxidant activity of chalcones and its spiro-heterocyclic analogues. *Chin J Org Chem* 2012;**32**:2141–7.
 79. odorova IT, Batovska DI, Stamboliyska BA. Evaluation of the radical scavenging activity of a series of synthetic hydroxychalcones towards the DPPH radical. *J Serb Chem Soc* 2011;**76**:491–7.
 80. Raghavan S, Manogaran P, Venkatraman G. Synthesis and anticancer activity of chalcones derived from vanillin and isovanillin. *Med Chem Res* 2015;**24**:1–9.
 81. Dahae L, Ki Hyun K, Sung Won M. Synthesis and biological evaluation of chalcone analogues as protective agents against cisplatin-induced cytotoxicity in kidney cells. *Bioorg Med Chem Lett* 2015;**25**:1929–32.
 82. Rao YK, Fang SH, Tzeng YM. Synthesis and biological evaluation of 3',4',5'-trimethoxychalcone analogues as inhibitors of nitric oxide production and tumor cell proliferation. *Bioorg Med Chem* 2009;**17**:7909–14.
 83. Bhat BA, Dhar KL, Puri SC. Synthesis and biological evaluation of chalcones and their derived pyrazoles as potential cytotoxic agents. *Bioorg Med Chem Lett* 2005;**15**:3177–80.
 84. Lopez SN, Castelli MV, Zacchino SA, Dominguez JN, Lobo G, Charris-Charris J, et al. *In vitro* antifungal evaluation and structure-activity relationships of a new series of chalcone derivatives and synthetic analogues, with inhibitory properties against polymers of the fungal cell wall. *Bioorg Med Chem* 2001;**9**:1999–2013.
 85. Yamali C, Ozgun DO, Gul HI. Synthesis and structure elucidation of 1-(2,5/3,5-difluorophenyl)-3-(2,3/2,4/2,5/3,4-dimethoxyphenyl)-2-propen-1-ones as anticancer agents. *Med Chem Res* 2017;**26**:1–9.
 86. Srinivasan B, Johnson TE, Lad R, Xing C. Structure–activity relationship studies of chalcone leading to 3-hydroxy-4,3',4',5'-tetramethoxychalcone and its analogues as potent nuclear factor κ B inhibitors and their anticancer activities. *J Med Chem* 2009;**52**:7228–35.
 87. Ivanova AB, Batovska DI, Todorova IT, Stamboliyska BA, Serly J, Molnar J. Comparative study on the MDR reversal effects of selected chalcones. *Int J Med Chem* 2011;**2011**:530780–7.
 88. Gu XH, Yu H, Jacobson AE, Rothman RB, Dersch CM, George C, et al. Design, synthesis, and monoamine transporter binding site affinities of methoxy derivatives of indatraline. *J Med Chem* 2000;**43**:4868–76.
 89. Pathak V, Ahmad I, Kahlon AK. Syntheses of 2-methoxyestradiol and eugenol template based diarylpropenes as non-steroidal anticancer agents. *RSC Adv* 2014;**4**:35171–85.

90. Mikulski D, Górnjak R, Molski M. A theoretical study of the structure-radical scavenging activity of *trans*-resveratrol analogues and *cis*-resveratrol in gas phase and water environment. *Eur J Med Chem* 2010;**45**:1015–27.
91. Braca A, Sortino C, Politi M, Morelli I, Mendez J. Antioxidant activity of flavonoids from *Licania licaniaeflora*. *J Ethnopharmacol* 2002;**79**:379–81.
92. Schmittgen TD, Livak KJ. Analyzing real-time PCR data by the comparative C_T method. *Nat Protoc* 2008;**3**:1101–8.
93. Xu HL, Mao KL, Lu CT, Fan ZL, Yang JJ, Xu J, et al. An injectable acellular matrix scaffold with absorbable permeable nanoparticles improves the therapeutic effects of docetaxel on glioblastoma. *Biomaterials* 2016;**107**:44–60.
94. Himori N, Watanabe H, Akaike N, Kurasawa M, Itoh J, Tanaka Y. Cerebral ischemia model with conscious mice: involvement of NMDA receptor activation and derangement of learning and memory ability. *J Pharmacol Methods* 1990;**23**:311–27.